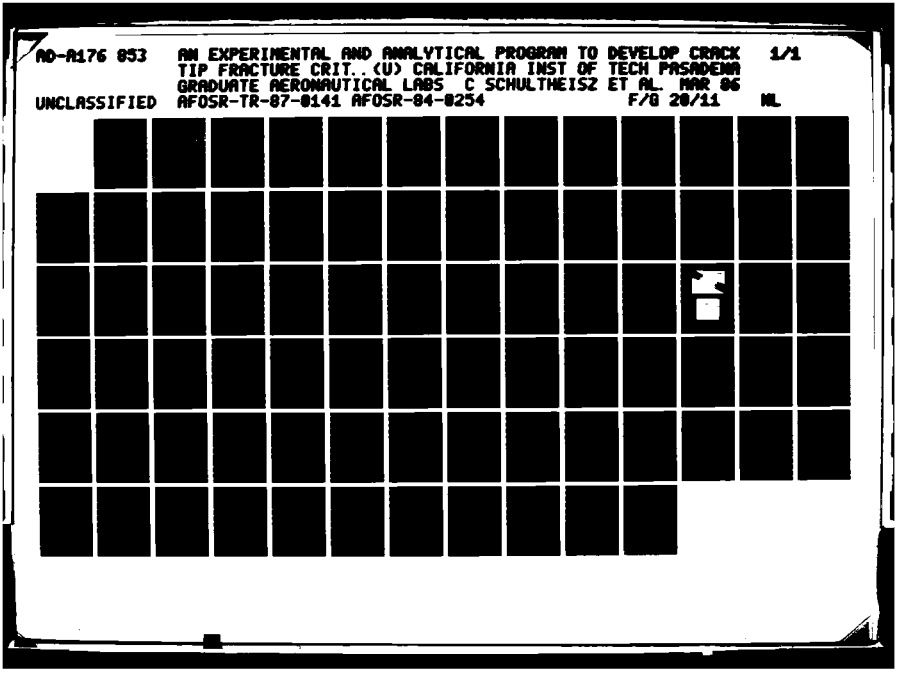
AD-A176 853 AN EXPERIMENTAL AND ANALYTICAL PROGRAM TO DEVELOP CRACK 1/1
TIP FRACTURE CRIT..(U) CALIFORNIA INST OF TECH PASADENA
GRADUATE AERONAUTICAL LABS C SCHULTHEISZ ET AL. MAR 86
UNCLASSIFIED AFOSR-TR-87-0141 AFOSR-84-0254 F/G 20/11 NL

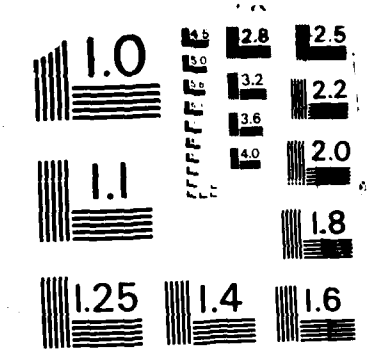

UNCLASSIFIED
SECURITY CLASSIFICATIC

REPORT DOCUMENTATION PAGE

1a. REPORT SECURITY CLASSIFICATION: unclassified	1b. RESTRICTIVE MARKINGS
2a. SECURITY CLASSIFICATION AUTHORITY	3. DISTRIBUTION / AVAILABILITY OF REPORT: Approved for public release; distribution unlimited.
2b. DECLASSIFICATION / DOWNGRADING SCHEDULE	
4. PERFORMING ORGANIZATION REPORT NUMBER(S)	5. MONITORING ORGANIZATION REPORT NUMBER(S): AFOSR-TR- 87-0141
6a. NAME OF PERFORMING ORGANIZATION: California Institute of Technology; 6b. OFFICE SYMBOL (If applicable)	7a. NAME OF MONITORING ORGANIZATION: AFOSR/NA
6c. ADDRESS (City, State, and ZIP Code): 1201 E. California Blvd. Pasadena, CA 91125	7b. ADDRESS (City, State, and ZIP Code): Building 410 Bolling AFB D.C. 20332-6448
8a. NAME OF FUNDING / SPONSORING ORGANIZATION: AFOSR; 8b. OFFICE SYMBOL (If applicable)	9. PROCUREMENT INSTRUMENT IDENTIFICATION NUMBER: AFOSR-84-0254
8c. ADDRESS (City, State, and ZIP Code): Building 410 Bolling AFB D.C. 20332-6448	10. SOURCE OF FUNDING NUMBERS: PROGRAM ELEMENT NO. 61102F; PROJECT NO. 2302; TASK NO. B2; WORK UNIT ACCESSION NO.

11 TITLE (Include Security Classification)
An Experimental and Analytical Program to Develop Crack Tip Fracture Criteria - Unclassified

12 PERSONAL AUTHOR(S)
C. Schultheisz, T. Ungsuwarungsri, W.G. Knauss

13a TYPE OF REPORT	13b. TIME COVERED	14. DATE OF REPORT (Year, Month, Day)	15. PAGE COUNT
Annual Report	FROM April '85 TO Dec. '85	March 1986	78

16 SUPPLEMENTARY NOTATION

17 COSATI CODES			18 SUBJECT TERMS (Continue on reverse if necessary and identify by block number)
FIELD	GROUP	SUB-GROUP	

19 ABSTRACT (Continue on reverse if necessary and identify by block number)

A summary of progress on the development of instrumentation to determine with great accuracy the in-plane and out-of-plane surface deformations in the vicinity of a crack tip. The purpose is to establish a data base for a) guiding theoretical research in characterizing the deformation fields in the crack tip vicinity for fracture research and b) to provide factual information for the evaluation of currently proposed theories dealing with crack tip deformation. The experimental tools under development are (D. Post's) moire interferometry for the in-plane deformations and optical interferometry for the out-of-plane ones. An essential part of this work is the implementation of a computer-based data processing unit, which is able to record and process in nearly real time fringe patterns into strain fields, and, for known - or estimated - constitutive behavior into stress fields. This report summarizes the state of developments and establishes that it is in phase with projected progress.

20 DISTRIBUTION / AVAILABILITY OF ABSTRACT	21 ABSTRACT SECURITY CLASSIFICATION
☒ UNCLASSIFIED/UNLIMITED ☐ SAME AS RPT ☐ DTIC USERS	unclassified
22a NAME OF RESPONSIBLE INDIVIDUAL: Maj. George Haritos	22b TELEPHONE (Include Area Code): (202)767-4935; 22c OFFICE SYMBOL: NA

DD FORM 1473, 84 MAR — 83 APR edition may be used until exhausted. All other editions are obsolete.

SECURITY CLASSIFICATION OF THIS PAGE

577 - L

Annual Progress Report on a Research Program

Grant No. AFOSR-84-0254

Entitled

AN EXPERIMENTAL AND ANALYTICAL PROGRAM TO DEVELOP CRACK TIP FRACTURE CRITERIA

by

C. Schultheisz*, T. Ungsuwarungsri*, and W.G. Knauss

April 1985 - December 1985

Graduate Aeronautical Laboratories
California Institute of Technology
Pasadena, California 91125

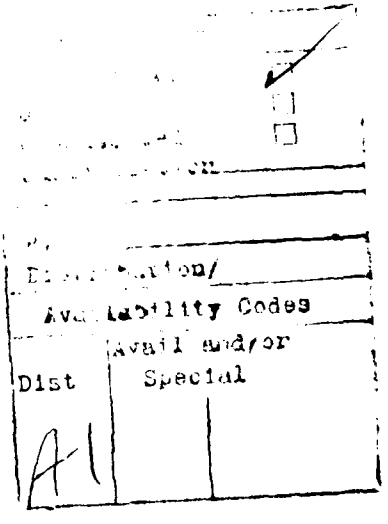

* Graduate Research Assistant.

** Professor of Aeronautics and Applied Mechanics.

ABSTRACT

Fracture mechanics has traditionally meant characterizing the linearly elastic response through stress intensity factors. However, it is recognized that fracture depends strongly on non-linear material behavior in a small region about the crack tip. New experimental and analytical investigations must make an effort to characterize this nonlinear behavior.

With this observation in mind, we are attempting to experimentally investigate the deformation field (and then calculate the strain and stress fields) at the tip of a crack. The experimental technique, Moire Interferometry, measures in-plane displacements and is sensitive to displacements on the order of microns. We are now constructing an interferometer which will measure both of the two linearly independent planar displacement components simultaneously; the out of plane deformation can also be determined on the same specimen using a Michelson Interferometer with similar sensitivity.

Much of the data acquisition and reduction will be carried out by computer through digital image processing. The computer can be used to compare measured behavior with analytical or numerical predictions and help to improve such models. We have purchased the image processing system and are integrating the components. It will be necessary to write specialized software to do the planned data reduction, but automating the data processing will eventually enable us to examine more results more thoroughly than could be done by hand.

We have also investigated the nonlinear material behavior (strain softening) numerically using two different models. The first is a model of a double cantilever beam crack specimen as a beam on a nonlinear foundation. The second is a model for the behavior of nonlinear crazing. Both of these models have been checked out on the two-dimensional problem and were the precursor to the problem of crack growth resulting from strain softening material behavior which follows classically plastic behavior.

1. INTRODUCTION

The fact that a crack exists in a body dominates the nature of the linearly elastic stress distribution near the tip of that crack. This notion of "crack tip autonomy" (with its universal inverse square root singularity) has traditionally left only the calculation of the strength of the singularity (Stress Intensity Factor) as the main effort of fracture mechanics research. The stress intensity factor is a function only of the geometry and magnitude of the applied loading, and is independent of material properties (for an isotropic linearly elastic solid).

The stress intensity factor does describe the conditions near the crack tip fairly well for many applications, such as fatigue. However, it has been recognized that the stress response at the tip of the crack must be nonlinear for all but the most brittle of materials, since the stresses predicted within the linearized theory of elasticity are singular, the material at the crack tip must act in some way to mitigate the effect of the stress singularity through plastic deformation.

There are several analytical models of the nonlinear (plastic) behavior at the crack tip, from the simple Dugdale-Barenblatt cohesive zone model to the power law hardening model of Hutchinson, Rice and Rosengren. Along with high speed computers have come numerous finite element and other numerical approximations. These models make assumptions and predictions about the nature of materials and their fracture response which must be tested under real conditions. In order to test the validity of the models, actual displacement, strain and stress distributions must be determined experimentally and compared with the predictions. It is also important to determine the extent to which a basic assumption, that the material is a continuum, is valid; fracture, at its core, is an interatomic process and hence a discrete process. Finite element models attempt to investigate the crack tip region by resorting to smaller and smaller elements, each having the properties of the continuum material, but it is obvious that there is a scale beyond which this discretization cannot be justified.

With these goals in mind, we are attempting to measure with high sensitivity the in-plane as well as the out-of-plane displacement field in the region of the crack tip. Once the displacement field is known, the strain field can be calculated from the displacement gradients and the stress field calculated from an assumed constitutive law. These

measurements can be used both to validate numerical predictions and as a source for actual physical input in order to improve the current numerical models. Our measurements will be performed through Post's method called Moire Interferometry, which measures relative in-plane displacements over an entire field. The displacements are revealed as fringes, contours of constant displacement relative to any other point in the field.

Since each measurement will generate an entire field of displacement information, it is necessary to process this data efficiently. A video digitizing system will thus be used to convert the fringe fields into a position-intensity array within a computer. The computer will then convert the fringe information to a position-displacement array, which can be compared with numerical or analytical preditions. The computer can also calculate the displacement gradients numerically and create a position-strain array. With an assumed constitutive law the strains can be converted to stresses.

2. EXPERIMENTAL PROCEDURES

Moire Interferometry is a highly sensitive experimental technique which measures in-plane relative displacements at the surface of a specimen. These displacements are inferred through the change in the diffraction angle of a laser beam as a diffraction grating deforms. The diffraction grating is a high frequency periodic profile variation of a reflective surface. The diffraction angle of the laser beam depends on the wavelength of the grating and, as the grating deforms, the grating wavelength changes and so does the diffraction angle. By using two laser beams from opposite directions, very small changes in the diffraction angles can be detected by observing the fringe pattern resulting from the interference the two diffracted laser beams. In fact, it can be shown that each of the interference fringes corresponds to a contour of constant relative displacement of the diffraction grating. The displacement increment between adjacent fringes is half the initial (undeformed) wavelength of the diffraction grating. The grating we plan to use has a wavelength of about 1.7 microns.

The required diffraction gratings are originally produced on high resolution photographic plates such as those used in holography. A thin coating of aluminum is evaporated onto the surface of the plate to increase the reflectivity. This reflective coating and the

grating profile can then be transferred to any flat surface with an adhesive such as epoxy. We have produced compact tension fracture specimens in this way, and this method can be used on flat plate specimens of any size and composition. Alternatively, it is possible to apply a photoresist to the specimen itself and produce a grating directly on the specimen in the same way as on a photographic plate. This should produce a better quality grating, but it limits the size and composition of the specimen since the photoresist must be developed in a chemical bath.

It is necessary to hold two laser beams fixed in pace for each component of displacement to be measured. We are constructing an interferometer which can measure two independent in-plane displacements simultaneously. As with any interferometric measurement system, vibrations introduce noise to the fringe pattern; we hope to eliminate this problem by mounting the interferometer and specimen loading device on a vibration isolated optical table.

The interferometer itself uses three laser beams which intersect at the surface of the specimen. Each beam comes from one corner of a square which is parallel to the specimen. By examining the interference between alternate pairs of intersecting laser beams, three different in-plane displacement components can be measured: 0, 45, and 90 degrees. (Of course one of these components can be derived from the other two.) Each laser beam must originate from the same source and all must travel paths of similar length to the specimen surface in order to obtain high contrast interference patterns.

Since each fringe represents a contour of constant displacement, as displacement gradients become high, so does the fringe density. This could create a problem, particularly for specimens exhibiting highly plastic deformations. However, with good photographic equipment we expect to be able to resolve 100 fringes/millimeter which corresponds to a strain of about 1% for the grating already described. This is most likely adequate for most metals. However, a coarser grating can allow for higher strain levels, and the displacement sensitivity can be reduced through holographic techniques, if that need arises very close to the crack tip.

At this time the machinery for the production of gratings on holographic plates is in place, as is the vacuum chamber for applying the reflective aluminum coatings. We are able to produce satisfactory diffraction gratings in this manner. The process of transferring the

gratings to a specimen with an adhesive has been tested and seems workable, the major difficulty being air bubbles in the adhesive causing local faults in the bond. All of the components of the three beam interferometer are here and the table top loading device is now available. It will require some time to assemble and align the interferometer since precise alignment is the most important part of any interferometric measurement system.

We expect to have the interferometer set up and some preliminary photographs of fringe patterns within the next six months. We can then decide if we need to explore alternative specimen geometries or different grating preparation methods. Then we can begin to characterize the displacement fields as a function of load, material properties and crack geometry.

3. COMPUTER SYSTEM

We have purchased a computer to automate the reduction of the data contained in the interference fringes. The computer itself is a Digital Equipment Corporation LSI 11/73 central processing unit with 4 megabytes (MB) of random access memory and an additional 180 MB of disk storage space. We also have a 70 MB tape cartridge drive for permanent storage.

The fringe patterns are input to the computer system by digitizing a video image: the analog video signal is converted to a digital representation by an Imaging Technology Incorporated Analog Processor and sent along the high speed video bus to the Imaging Technology Incorporated Frame Buffer where it is stored as an x-y position with a corresponding brightness level. We have the ability to convert a photograph to an array of 1024x960 positions with 256 brightness levels. At this resolution, each picture occupies about one megabyte of memory storage space. This system has been assembled and some basic software to transfer images from the frame buffer to the computer memory and vice versa has been written.

The next work item concerns the development of software to enhance and analyze the fringe patterns. The enhancement consists mainly of filtering out noise and thresholding the image to reduce the fringes to thin black lines on a white background instead a variation of gray levels. Next, a program to trace the position of the fringes with respect to the

crack tip will be needed. This part of the process will require some human interaction to impose a coordinate system and to assign a displacement value to each fringe according to the boundary conditions imposed. These programs should also be availale to us within the next six months. The displacement field calculated can then be compared to an analytically generated displacement field at each point in the image array.

Calculation of the strain field in two or three-dimensions is straight forward in principle once the displacement field is known; however, differentiation can be troublesome as it amplifies non-smooth features in the field. On the other hand, this amplification may indicate regions where continuum as constitutive law, the stress field may be calculated. We shall first consider classical plasticity theories such as power-law strain hardening models to determine the stress fields. Imposing equilibrium will also help indicate whether the constitutive assumptions are valid.

Although the initial emphasis will be on the two-dimensional behavior of the field quantities, we expect to proceed to the study of three-dimensional effects in a similar way. These effects depend strongly on the thickness of the specimen as well as the similarity of the crack geometry through the thickness. Numerical calculations allowing for three-dimensional effects are also being undertaken.

4. ANALYTICAL EFFORT

4.1. Background.

Analytical studies in elastic-plastic fracture mechanics have been mainly directed at identifying certain fracture parameters such as the J-integral, the crack tip opening displacement or angle. Although this approach has been widely adopted and applied with some success in predicting the behavior of stable crack growth (e.g. using the J-resistance curve), it fails to provide a framework for studying in further depth the effects of the failure mechanisms in the crack tip zone on the global behavior of crack growth. Specifically, we do not fully understand how damage-induced softening behavior of the crack tip material - which varies in characteristics with the microstructural failure mechanisms - affects the stability of the crack itself. In metals, cracks advance with varying

degrees of ductility depending on the loading and on the environmental conditions. If the fracture is relatively brittle, the crack surfaces separate easily and little plastic deformation is incurred in the material surrounding the crack path. On the other hand, when the crack faces are formed through void nucleation, growth and coalescence, the effective surface energy turns out to be substantially higher than the brittle surface energy; also the extent of plastic deformation in the material adjacent to the path traversed by the crack is much greater. Thus, the material toughness and separation characteristics reflecting the failure mechanisms at the crack tip directly control the energy expenditure and the stress and strain fields around the crack front. Seen in this light, it is clear that fracture analyses are necessarily incomplete without incorporating the proper separation laws which describe the failure modes at the crack tip; in spite of the fact that one-parameter fracture criteria serve and have served very useful purposes they seem to be of somewhat limited virtue for understanding fracture as a fundamental process. The research we conducted thus far has been focused on these aspects of fracture discussed above. Our attempts have been confined to planar geometry (two-dimensional problem) with extension to the fully three-dimensional case in mind.

Two pilot problems, analyses of the fully nonlinear cohesive zone model of the Barenblatt-Dugdale type, have been studied in detail. The first problem is a beam on nonlinear foundation analysis appropriate for a double cantilever beam (DCB) specimen whose material is elastic with the nonlinear damage-softened material confined to a thin boundary layer on the crack plane [1]. The second problem concerns a nonlinear craze embedded in an elastic medium subjected to symmetrical loading. The nonlinearity is again confined to the craze fibril material [2]. These two analyses yield a number of interesting findings suggesting that the damage-induced softening material behavior at the crack tip plays a central role in determining the global behavior of crack propagation.

5. CURRENT RESEARCH

We now extend our study to the case where the material surrounding the crack is not simply elastic. The first problem we examine consists of a compact tension specimen loaded by a displacement controlled machine. The material is elastic-plastic described by a J_2 -flow theory. The specimen is modeled by a finite element mesh while the damage-

softened boundary layer along which the crack propagates is represented by a row of non-linearly softening springs. The springs' initial stiffness is simply the material Young's modulus, and the onset of softening occurs when a critical nodal force is reached and failure takes place at a critical separation distance. The "surface energy" is equal to the area under the spring's separation characteristics; material toughness would include the energy dissipated in plastic deformation. Note that the definition of the problem is complete and no extra fracture criterion is needed.

The finite element program ABAQUS is employed for this purpose. Preliminary studies indicate that the extent of crack growth is critically dependent on the critical (threshold) nodal forces and on the intial "softening" slope of the spring.

More detailed studies are being undertaken and should resolve some of the difficulty currently encountered such as the proper scaling of the springs when going from a coarser mesh to a finer one. Early tests indicate that the scaling is nonlinear and may have to be obtained by trial and error. Finally, the nonlinear spring technique can be used in dynamic (not necessarily steady state) problems as well.

6. REFERENCES

Details on the pilot study of non-linear craze response on the stability of a craze/crack combination are attached to this report.

1. Ungsuwarungsri, T. and Knauss, W.G., "The Role of Damage-Softened Material Behavior on Toughness and Fracture in Composites and Adhesives," GALCIT SM Report 85-4, California Institute of Technology, Pasadena, CA 1985.

2. Ungsuwarungsri, T. and Knauss, W.G., "A Nonlinear Analysis of an Equilibrium Craze in an Infinite Medium sublected to Symmetrical Loading," GALCIT SM Report 85-15, California Institute of Technology, Pasadena, CA 1985.

APPENDICES

SM 85-15-1

A NONLINEAR ANALYSIS OF AN EQUILIBRIUM CRAZE
PART I: PROBLEM FORMULATION AND SOLUTION

by

T. Ungsuwarungsri* and W.G. Knauss**

Graduate Aeronautical Laboratories
California Institute of Technology
Pasadena, CA 91125

---

* Graduate Research Assistant

** Professor of Aeronautics and Applied Mechanics

ABSTRACT

This study investigates the effect of nonlinear cohesive forces on crack growth with the special problem of craze mechanics in mind. The work is presented in two parts. In the first and present one, we develop a numerical method for determining the equilibrium shape of a craze in an infinite elastic plane whose fibrils exhibit very general nonlinear force-displacement (P-V) behavior, including strain softening characteristics. The second part of this study [1][1] deals with the numerical simulation of craze and crack growth.[2]

The problem formulation is based on the superposition of the relevant elasticity Green's function and the solution for the resulting nonlinear problem is effected by using Picard's successive approximation scheme. Both field equilibrium and the Barenblatt condition for vanishing stress and strain singularities are satisfied simultaneously, rendering the craze tip profile cusp-like. The formulation allows the stress distribution profile and the corresponding P-V relation to be computed from experimentally measured craze/crack displacement contours with certain advantages over other methods proposed to date; it allows also the computation of the craze or crack/craze profile if the P-V relation, far-field load and craze or crack size are specified. Numerical investigations indicate that only certain classes of the fibril P-V relations are consistent with measured craze profiles. In addition, it is found that for a given P-V relation, nontrivial solutions exist only for certain ranges of craze lengths depending on the P-V characteristics under consideration.

1. The references are listed at the end of the paper.

2. The unabridged version of these two papers is given in reference 2.

1. INTRODUCTION

When glassy polymers are subjected to extensional strains larger than about 0.2%, tney begin to exhibit local 'plastic' deformation. Two distinct processes of plastic deformations have been observed, one being mainly a shearing phenomenon such as diffuse shear yielding and localized shear band formation, and the other being caused by cavitation and void growth commonly called 'crazing'. The latter process is characterized by a loss of intermolecular cohesion, molecular flow and orientation as well as a significant decrease in local density [3]. In this work, we shall concern ourselves only with the phenomenon of crazing.

The subject of crazing has been extensively studied by both material (polymer) scientists and applied mechanicians. Literature addressing various aspects of crazing can be found in references 3 through 10. We shall discuss here briefly the pertinent physical concepts and the motivations leading to the present investigation.

It has been recognized for some time that fracture in thermoplastic polymers is usually preceded by the formation of crazes. Crazes are formed in the bulk polymer along planes normal to the direction of maximum principal tensile stress; they tend to nucleate at micro-defects or inclusions and grow by the formation of fibrils from the bulk polymer [6,7] and thicken through a combination of two distinct mechanisms, namely through 'surface drawing' and 'creep'. In surface drawing, new polymer is drawn from the bulk into the craze in the form of fibrils. During creep existing fibrils are simply elongated, mostly locally around the weak portions. Note that although 'creep' implicitly signifies a time dependent process, we will exclude time consideration from this work.[3] For our purpose it is sufficient to recognize that the interplay of these two mechanisms gives rise to an effective force-displacement (P-V) behavior which we consider

3. For an analysis accounting for these two basic mechanisms, see the recent paper by Kramer and Hart [11].

to be initially prescribed. Here 'force' represents the cohesive stress exerted by the fibril on the craze/bulk polymer boundary. 'Displacement' refers to the net displacement of the craze boundary (see Section 2.1 for details).

Electron microscopy shows that the typical craze thickness is on the order of 1 μm and the length to thickness (aspect) ratio is approximately 10^2 to 10^3. Crazes generally consist of a network of fibrils between 10 to 40 nm in diameter, interspersed with voids of similar dimensions. The transition boundary between a craze and the bulk polymer where surface drawing takes place is very thin i.e. less than 2 nm. Craze fibrils have been shown to exhibit considerable strength [8,9]. Therefore, crazing could, under certain conditions, substantially enhance the toughness of bulk polymers. However the presence of crazes does not necessarily enhance the strength of the overall structure. In many instances, uncontrolled craze growth tends to induce fracture, causing structures to fail 'prematurely'. For more in-depth discussions on microstructures and properties of crazes, see references 7 and 10. Figure 1 shows a typical craze and its tip region.[4]

We next review briefly the analytical approaches that have been attempted in modelling the crazing phenomenon to date. Barenblatt considered the problem of equilibrium cracks in brittle fracture [12]; even though the analysis was carried out in the context of cracks, the basic propositions and concepts apply to crazes equally well. His proposition eliminates the infinite stresses and strains at the crack tip by incorporating cohesive stresses distributed over a cohesive zone of finite length such that the crack is in "equilibrium" and the stress intensity factor vanishes. Assuming a constant cohesive (yield) stress in this cohesive zone, Dugdale derived a simple relationship between its size and the applied stress [13] in plane stress; this study was then considered by

4. The micrographs were taken by L. Berger and made available to us by Professor E.J. Kramer.

Rice in more detail using the rigid-plastic strip model [14]. Goodier and coworkers calculated the rate of plastic work dissipation for the same model with an added assumption that a crack propagates with a self-similar geometry [15] and later introduced a crack propagation model using non-linear atomic separation laws indicating how the cohesive stress distribution changed as the crack extended [16]. Atkinson proposed an iterative scheme for solving axially symmetric problems relating to cracks that open under a displacement-dependent internal stress without, however, satisfying the Barenblatt condition [17]. Andersson and Bergkvist solved a crack problem using a strip model [18]: Their strip material behavior was piecewise-linear with a "linear softening" characteristic; the strip extended to infinity and the displacements decreased gradually to zero, so that the stresses were bounded everywhere, similar to those in reference 16. E. Smith derived a class of acceptable force-displacement relationships by starting with displacement profiles chosen so as to yield simple solutions to the integral equation which relate the displacement and stress within the cohesive zone [19] under satisfaction of Barenblatt's boundedness condition.

In addition to these stress analyses, there are a number of contributions concerned with the mechanics of craze growth. In 1965, Knight [20] employed the Fourier transform method [21] to calculate the stress distribution along a craze, but due to the erroneous craze profile used, the resulting stress distribution was incorrect. Knauss presented a boundary-layer model (formulated for a semi-infinite crack) which is extendable to account for rate-dependent cohesive stress-displacement behavior [22]. The critical strain (displacement) criterion was employed and it was found that for materials with softening force-displacement characteristics, the crack tip cohesive stress decreased rapidly to zero while the size of the cohesive zone rose sharply as the critical strain was approached at the crack tip.

Verheulpen-Heymans and Bauwens presented a modified Dugdale model with a constant cohesive stress acting over a short distance behind the craze tip and a lower constant cohesive stress acting over the rest of the craze length [23]. Lauterwasser and Kramer performed experiments in which accurate measurements of the density of the craze materials together with the craze profile permitted the determination of the stress distribution profile [7] through use of the Fourier transform technique [21]. They also demonstrated conclusively that surface drawing was the dominant process in craze thickening. As we shall see later, this finding is of general significance in determining the appropriate P-V relations for craze fibrils. Subsequently, Wang and Kramer employed a distributed dislocation model to calculate the far-field applied stress as well as the surface stress profile along the craze from the experimental displacement profile in the craze zone [24]. The method gave results in good agreement with the Fourier transform method. The stress profiles obtained in this way for polystyrene and polycarbonate exhibited stress concentrations at the crack tip as well as at the craze tip and approximately constant stress in between. Donald and Kramer later examined four additional polymers and obtained similar results [25].

Attempts to determine stress distribution profiles for given displacement profiles by using other methods such as finite element and boundary element analyses were made by Bevan [26] and Sun and Hsiao [27], where the latter authors also allowed yielding in the bulk polymer in their finite element study. Although the results of both studies agreed generally with those obtained by Kramer et al [7] through the Fourier transform method, the accuracy and efficiency seems wanting.

So far we have reviewed studies in which the stress distribution along the craze boundary is calculated from the experimental displacement profile by using various analytical techniques. The main purpose of the present study is, however, to address the more difficult problem where one seeks solutions for both the stress and displacement profiles together with the far-field applied stress, given a craze length and a nonlinear

fibril P-V relation, such that Barenblatt's condition is also satisfied. This problem has thus far not been solved correctly. Recently, Walton and Weitsman presented a solution scheme for the special case in which the fibril P-V relation is linear [28] and later Weitsman [29] extended that analysis to include the case where the P-V relation is nonlinear. The analyses in references 28 and 29 are, however, deficient in several aspects. For instance, their solution did not satisfy the Barenblatt condition but had to be 'corrected' later by imposing additional cohesive stresses in a small 'tip zone' to make the stress intensity vanish. This correction is artificial and results in stress distributions that are inconsistent with those deduced from experiments [24,25]. This shortcoming is due partly to an inapropriate choice for the fibril P-V behavior; interested readers may wish to consult reference 2 for a more complete discussion.

In view of these past contributions, it becomes clear that an analytical and computationally efficient method for determining the displacement and stress profiles of a craze with prescribed nonlinear fibril behavior under satisfaction of both equilibrium and the smooth-closure conditions is still lacking. The primary objective of this work is to present such an analysis and to use it in the study of various aspects of the mechanics of craze and crack growth in thermoplastic materials.

In the following sections, we discuss the model for representing a craze. The idealizations made to model the problem are explained in Section 2.1. The mathematical formulation including nondimensionalization and discretization for final implementation then follow in Sections 2.2 and 2.3. In Section 3, two alternate methods for computing stress distribution profiles from craze displacement contours are presented for the case of a full craze and for a craze with a central crack. Because of their simplicity, these methods are both computationally more efficient and inherently more accurate (for the same degree of discretization) than those used in the past by other investigators. The convergence characteristics of the solution technique are briefly explored and the general

applicability and performance of the numerical schemes are assessed in Section 4.1. Some characteristics of the fibril P-V relations that are inconsistent with realistic craze profiles are then examined and the existence of solutions is addressed briefly in Section 4.2. The question of the uniqueness of solutions is raised but not addressed rigorously.

2. PROBLEM FORMULATIONS AND SOLUTIONS

In this section, we reduce the physical problem to a mathematically manageable one through suitable approximations. The resulting equations are then nondimensionalized and solved through a numerical algorithm based on Picard's iteration.

2.1. Geometric and Mathematical Idealization.

We consider first the geometry of the problem as depicted in Figure 2a. A craze of length C with an (internal) central crack of length A is embedded in an infinite plate subjected to a remote and uniform tensile stress Σ_∞ applied normal to the major axis of the craze. X,Y are the coordinates and W(X) denotes the Y-displacement of the craze contour. We let P(X) represent the cohesive force (stress) distribution exerted by the fibrils.

As shown by Lauterwasser and Kramer, a craze is formed from a primordial craze, characterized by a contour $W_o(X)$: this contour contains the bulk polymer material which is subsequently transformed into craze fibrils through the surface drawing process [7]. Thus the dashed contour $W_o(X)$ in Figure 2b is displaced in the drawing process to the solid contour W(X) due to the application of Σ_∞. Since we know from experiments that $W_o(X)$ is much smaller than C and that the slope, $W'_o(X)$, is also very small everywhere, we can recast the geometry of the problem as shown in Figure 2c where V(X) is the net displacement of the craze profile caused by the applied stress as measured from $W_o(X)$ so that $V(X) = W(X) - W_o(X)$. Cast

in this light, the force-displacement (P-V) relation may be represented schematically as shown in Figure 2d. Keeping in mind that $V < 0$ corresponds to the primordial craze under small strain prior to fibrillation, the dashed portion of the P-V curve is assumed linear with a slope equal to Young's modulus, E, for the bulk polymer. At $V = 0$, the threshold (or fibrillation) stress P_o is reached and from then on the P-V relation is nonlinear. Three P-V relations are illustrated, curve #1 is representative of a craze that does not contain a crack. We shall later refer to such a craze as a 'full craze'. Curve #2 allows for continued hardening before softening to failure (fibril degradation and rupture) at V_c. Curve #3 is typical of a craze with a central crack; this rehardening behavior may be understood in the context of the midrib behavior [7].[5]

2.2. The Mathematical Formulation.

By superposing the Green's functions obtained through Westergaard stress function method [30], the solutions to the problem can be written as[6]

$$V(X) = \left(\frac{1+\eta}{4\mu}\right) \frac{1}{\pi} \int_o^C (\Sigma_\infty - P(T)) \log \left| \frac{\sqrt{C^2-X^2}+\sqrt{C^2-T^2}}{\sqrt{C^2-X^2}-\sqrt{C^2-T^2}} \right| dT \qquad (2.1)$$

$$K_I = 2\sqrt{\frac{C}{\pi}} \left[\int_o^C \frac{\Sigma_\infty - p(T)}{\sqrt{C^2-T^2}} dT \right] \qquad (2.2)$$

where $\eta = \left(\frac{3-\nu}{1+\nu}\right)$ for plane stress and $(3-4\nu)$ for plane-strain; ν = Poisson's ratio; μ = shear modulus. K_I is the mode-I stress intensity

5. The midrib is formed initially at the craze tip due to fibril drawing at high stress. As the craze grows, the midrib is unloaded as it becomes part of the mature (developed) craze. The introduction of a crack in the craze causes the stress at the crack tip to rise, so that the midrib is reloaded and therefore must sustain higher stress.

6. Huang independently employed an identical formulation in studying the size of the crack tip cohesive zone based on an interatomic potential [31].

factor, and V(X) is the net displacement due to the far-field loading and the fibril cohesive stress.

For presentation of the results, it is helpful to non-dimensionalize pertinent parameters. We let a craze length C_o be the reference length. The stresses are scaled by $(\frac{4\mu}{1+\eta})$; in this fashion, the Poisson's ratio is absorbed for both cases of plane stress and plane strain. In short,

$$\begin{aligned} C_{ref} &= C_o \\ \Sigma_{ref} &= \frac{E}{2} && \text{for plane stress} \\ &= \frac{E}{2(1-\nu^2)} && \text{for plane strain} \end{aligned}$$

We shall use lower case letters for dimensionless quantities and define

$$c \equiv \frac{C}{C_o}, \quad a \equiv \frac{A}{C_o}, \quad x \equiv \frac{X}{C_o}, \quad y \equiv \frac{Y}{C_o}$$

$$w \equiv \frac{W}{C_o}, \quad w_o \equiv \frac{W_o}{C_o}, \quad v \equiv \frac{V}{C_o}, \quad \tau \equiv \frac{T}{C_o}$$

and, $\sigma_\infty \equiv \frac{\Sigma_\infty}{\Sigma_{ref}}, \quad p \equiv \frac{P}{\Sigma_{ref}}$

Thus, in dimensionless forms, (2.1) and (2.2) are

$$v(x) = \int_o^c [\sigma_\infty - p(\tau)]\, m(c,x,\tau)\, d\tau \tag{2.3}$$

$$k_I = 2\sqrt{\frac{c}{\pi}} \left[\int_o^c \frac{\sigma_\infty - p(\tau)}{\sqrt{c^2-\tau^2}}\, d\tau \right] \tag{2.4}$$

where the kernel in equations (2.3) is given by

$$m(c,x,\tau) = \frac{1}{\pi} \log \left| \frac{\sqrt{c^2-x^2}+\sqrt{c^2-\tau^2}}{\sqrt{c^2-x^2}-\sqrt{c^2-\tau^2}} \right| \tag{2.5}$$

Note that here k_I is dimensionless. Integrating equation (2.3) yields

$$v(x) = \sigma_\infty \sqrt{c^2-x^2} - \int_0^c m(c,x,\tau)\, p(\tau)\, d\tau \qquad (2.6)$$

For the stress at the craze tip to be finite, or equivalently, for the craze tip to close smoothly, i.e. $v'(c) = 0$, it is necessary and sufficient that k_I vanish. Then (2.4) gives

$$\sigma_\infty = \frac{2}{\pi} \int_0^c \frac{p(\tau)}{\sqrt{c^2-\tau^2}}\, d\tau \qquad (2.7)$$

Substituting σ_∞ from (2.7) into (2.6), one obtains

$$v(x) = \int_0^c h(c,x,\tau)\, p(\tau)\, d\tau \qquad (2.8)$$

where

$$h(c,x,\tau) = \frac{2}{\pi} \left| \frac{\sqrt{c^2-x^2}}{\sqrt{c^2-\tau^2}} - m(c,x,\tau) \right| \qquad (2.9)$$

The formulation is completed by specifying the fibril force-displacement behavior

$$p(x) = p[v(x)] \qquad (2.10)^7$$

Equations (2.8) and (2.10) must be solved simultaneously. This is accomplished by using Picard's method of successive approximation outlined below[8]

---

7. The more general case, $p(x) = p[v(x),x]$ can be handled within the frame work of our formulation using the same solution scheme. A p-v relation with explicit dependence on x is a more realistic candidate; however due to lack of any such data, we confine our attention to the form (2.10).

8. As it turns out, this simple scheme is much more efficient than the Newton iterative scheme which was also implemented and yielded the same results.

We start with an initial guess of the form,

$$v^o(x) = \sigma_\infty^o (c - x)^r \tag{2.11}$$

where σ_∞^o and r are to be appropriately chosen; other forms of $v^o(x)$ are also acceptable.

The k^{th} approximation is given by

$$v^k(x) = \int_o^c h(c,x,\tau) p[v^{k-1}(\tau)] d\tau \; ; \quad k = 1,2,... \tag{2.12}$$

We consider that a solution has been attained when $v^k(x)$ differs from $v^{k-1}(x)$ at all (discretized) points by 0.1% or less. The convergence of the scheme is found to be relatively insensitive to the choice of the initial guess of σ_∞^o and r (see Section 3.1).

It is worth noting that in the case where a crack is present as determined by the critical crack tip opening displacement (CTOD) criterion (see [1] for further discussion), the crack length is not fixed a priori but is obtained as part of the solution. We next discretize the equations for numerical implementation.

2.3. Discretization and the Resulting Algorithm.

Because the kernels $m(c,x,\tau)$ and $h(c,x,\tau)$ defined by (2.5) and (2.9) can be evaluated in closed forms, the integration of these 'singular' integrals can be calculated very accurately without requiring excessive subdivisions of the domain.[9] We discretize the domain of integration into n equal intervals of length Δx , where

9. For contributions about the singular points, the Cauchy Principal values of the integrals are used.

$$\Delta x = \Delta\tau = c/n$$

and x_i, t_i, v_i, p_i are evaluated at the midpoint of each interval. With this in mind, an integral I(x) can be approximated as[10]

$$I(x_i) \equiv \int_0^c f(c,x_i,\tau)\ p(\tau)d\tau \equiv \bar{f}_j(c,x_i)p_j = \bar{f}_{ij}p_j \qquad (2.13)$$

where

$$\bar{f}_{ij} \equiv \bar{f}_j(c,x_i) \equiv \int_{\tau_j-\Delta\tau/2}^{\tau_j+\Delta\tau/2} f(c,x_i,\tau)\ d\tau \qquad (2.14)$$

Integrals of the form (2.14) in this study are easily evaluated in closed forms; specifically, from (2.5) and (2.6), one obtains

$$v_i = \sigma_\infty\sqrt{c^2-x_i^2} - \bar{m}_{ij}p_j \qquad (2.15)$$

where

$$\bar{m}_{ij} \equiv \frac{1}{\pi}\left\{ \tau \log\left| \frac{\sqrt{c^2-x_i^2}+\sqrt{c^2-\tau^2}}{\sqrt{c^2-x_i^2}-\sqrt{c^2-\tau^2}} \right| - 2\sqrt{c^2-x_i^2}\cos^{-1}\left(\frac{\tau}{c}\right) \right.$$

$$\left. + x_i \log\left| \frac{x_i\sqrt{c^2-\tau^2}-\tau\sqrt{c^2-x_i^2}}{x_i\sqrt{c^2-\tau^2}+\tau\sqrt{c^2-x_i^2}} \right| \right|_{\tau=\tau_j-\Delta\tau/2}^{\tau=\tau_j+\Delta\tau/2} \qquad (2.16)$$

Similarly, (2.7) may be written as

10. Repeated indices indicate summation from 1 to n.

$$\sigma_\infty = \int_0^c l(c,\tau)\, p(\tau)d\tau = \bar{I}_j p_j \tag{2.17}$$

where $l(c,\tau) = \frac{2}{\pi} \frac{1}{\sqrt{c^2-\tau^2}}$ and

$$\bar{I}_j \equiv \frac{2}{\pi}\left[\sin^{-1}\left(\frac{\tau}{c}\right)\right]_{\tau=\tau_j-\Delta\tau/2}^{\tau=\tau_j+\Delta\tau/2} \tag{2.18}$$

In view of (2.8) and (2.9), we obtain in compact form,

$$v_i \equiv v(x_i) \equiv \bar{h}_{ij} p_j \tag{2.19}$$

where

$$\bar{h}_{ij} \equiv \sqrt{c^2-x_i^2}\, \bar{I}_j - \bar{m}_{ij} \tag{2.20}$$[11]

It turns out that from equations (2.16), (2.18), and (2.20), $\bar{I}_j$ is independent of c while $\bar{m}_{ij}$ and $\bar{h}_{ij}$ are homogeneous in c. These properties prove to be very useful when we employ the numerical algorithm to study craze and crack growth in the second part of this work [1]. In concise form, one has

$$\bar{I}_j = \bar{I}_j(c,n) = \bar{I}_j(1,n) \tag{2.21}$$

$$\bar{m}_{ij} = \bar{m}_{ij}(c,n) = c \cdot \bar{m}_{ij}(1,n) \tag{2.22}$$

$$\bar{h}_{ij} = \bar{h}_{ij}(c,n) = c \cdot \bar{h}_{ij}(1,n) \tag{2.23}$$

Thus, for a given degree of discretization n , $\bar{I}_j$, $\bar{m}_{ij}$ and $\bar{h}_{ij}$ only need to be computed once for c=1 and stored for later use. In the simulation

11. Note that the matrix $\bar{h}_{ij}$ is singular i.e. given a displacement profile v(x), the cohesive stress profile can only be determined up to an additive constant. This, however, does not affect the validity of our algorithm.

of craze and crack growth [1], c increases continually, thus the properties exhibited in (2.21-2.23) reduce the computation time substantially. Note that $\bar{l}_j$, $\bar{m}_{ij}$ and $\bar{h}_{ij}$ are independent of the p-v relation considered.

The algorithm can now be summarized. Given a craze length c and a p-v relation, we seek solutions in the form of p(x), v(x) and σ_∞ according to the following procedure:

$$\text{Prescribed p-v relation :} \quad p(x_i) = p_i = p(v(x_i)) = p(v_i) \tag{2.24a}$$

$$\text{Initial guess :} \quad v^o(x_i) = v_i^o = \sigma_\infty^o (c-x_i)^r \tag{2.24b}$$

$$k^{th}\text{-iteration :} \quad v_i^k = v^k(x_i) = \bar{h}_{ij}(c,n)p(v_j^{k-1}) \tag{2.24c}$$

$$p_i^k = p(v_i^k) \tag{2.24d}$$

$$\sigma_\infty^k = \bar{l}_j p_j^k \tag{2.24e}$$

Convergence is considered achieved when the maximal change for any v_j is less than 0.1% between two successive iterations.

3. SCHEMES FOR DETERMINING STRESS PROFILES FROM DISPLACEMENT PROFILES

As mentioned in the introduction, for the case of a full craze, the stress distribution profile p(x) may be obtained from the measured displacement profile v(x) and σ_∞ using the Fourier transform method [21]. However, for a craze with a central crack, only the displacement profile in the craze zone is needed to determine both p(x) and σ_∞ using a distributed dislocation scheme [24]. Here we present two alternative methods for determining the stress profiles based on the formulation in the previous section; one method is suitable for a full craze, the other for a craze containing a central crack. Both schemes have been fully tested and found to be numerically more efficient than the methods previously

proposed [7,24,26].

First we discuss the method suitable for the problem of a full craze. Given $v(x_i)$ and σ_∞, equation (2.15) can be rewritten as

$$\bar{m}_{ij}p_j = (\sigma_\infty\sqrt{c^2-x_i^2} - v_i) \tag{3.1}$$

Equation (3.1) is a system of n linear equations from which p_j can be determined either by Gaussian elimination or by inverting $\bar{m}_{ij}$. In the latter case, (3.1) and (2.22) gives

$$p_j = \bar{m}^{-1}_{ij}(c,n)(\sigma_\infty\sqrt{c^2-x_i} - v_i) \tag{3.2}$$

where

$$\bar{m}^{-1}_{ij}(c,n) = \bar{m}^{-1}_{ij}(1,n)/c \tag{3.3}$$

Note that $\bar{m}^{-1}_{ij}(1,n)$ only needs to be computed once and stored for later use.

For demonstration purposes, this scheme is applied to $v(x)$ and σ_∞ as presented in reference 7 (see Figure 3). The resulting cohesive force distribution $p(x)$ shown in Figure 4 and that derived in [7] through the Fourier Transform method are virtually identical. The p-v relation obtained by combining Figures 3 and 4 is plotted in Figure 5.

This method is, of course, also applicable to a craze with an internal crack. However, since the measured displacement profiles in the crack region are usually not reliable on a point-by-point basis (see [24]), an alternative scheme using only the displacement profile in the craze zone as boundary data is preferable. Such a method has been presented by Kramer and Wang [24]; however, the method requires differentiation of the

experimentally measured displacement profile which incurs additional error. In view of this shortcoming, we present here a scheme which requires as inputs only the displacement v_j in the craze zone and the crack tip location. The outputs are the stress profile p(x), the applied stress σ_∞ and the displacement in the crack region.

Let i_t be such that the fibril cohesive force at the i^{th} station is

$$p_i = 0 \qquad \text{for} \qquad i < i_t$$
$$p_i \neq 0 \qquad \text{for} \qquad i \geq i_t \tag{3.4}$$

Given the displacement in the craze zone, v_i for $i \geq i_t$, we wish to find σ_∞ and p_i for $i \geq i_t$ and v_i for $i < i_t$. Consider equation (2.19),

$$v_i = \bar{h}_{ij} p_j \ , \qquad i,j = 1,2,\ldots,n \tag{2.19}$$

In light of (3.4), (2.19) reduces to

$$v_l = 0 \quad ; \qquad l = 1,2,\ldots,i_t-1 \tag{3.5a}$$

$$v_l = \bar{h}_{lk} p_k \ ; \qquad l,k = i_t, i_t+1,\ldots,n \tag{3.5b}$$

Equation (3.5b) can be solved for p_k, $k = i_t,\ldots,n$ by Gaussian elimination. Then by (2.17) and (2.19)

$$\sigma_\infty = \bar{l}_j p_j = \bar{l}_k p_k \ , \qquad k = i_t,\ldots,n \tag{3.6}$$

$$v_i = \bar{h}_{ik} p_k \ , \qquad i = 1,\ldots,i_t-1 \ \text{ and } \ k = i_t,\ldots,n \tag{3.7}$$

This completes the presentation of the two alternative schemes for computing p(x) from v(x).

4. THE CHARACTERISTICS OF THE ALGORITHM AND THE p-v RELATION

We examine next two aspects of the craze problem from a general viewpoint. First we report on the convergence characteristics of the algorithm and attempt to give some broad criteria on its applicability and effectiveness. Then two models of p-v relations are studied with the aim of determining how the existence of a solution depends on the nonlinearity of the p-v relation. The findings indicate that there are restrictions on the characters of the p-v relations if realistic craze profiles are to result, i.e. profiles with nonnegative (non-interpenetrating) displacements at all points.

4.1. The Convergence of the Algorithm.

Having discussed the algorithm and the convergence criterion in Sections 2.2 and 2.3, we consider the characteristics of the algorithm as applied to specific problems. In Figures 6, we show how the solution for v(x) for a (half-cosine) p-v relation[12] converges for an initial guess of the form

$$v^o(x) = \sigma_\infty^o (c - x)^r$$

where in this example, the initial guesses are $\sigma_\infty^o = 0.05$ and $r = 1.5$. Nine iterations are required for convergence in this case. (Each iteration takes about 1.2 CPU seconds on a VAX 11-780.) The solution for σ_∞ is 0.0176. Again, a displacement tolerance of 0.1% is used as the convergence criterion. For n=200, we find that checking for convergence at only 20 or 100 equi-spaced points give identical results to checking at all 200 points. This is so because the convergence is quite uniform for most p-v relations. Throughout this work, we conservatively use 100 checkpoints for n=200.[13]

12. Specifically, the p-v relation in Figure 7(b) with $p_o = p_m = 0.0393$, $v_m = 0.0$ and $v_c = 0.008$ is used.

With regard to the general applicability of the algorithm, we find that the initial guess does not need to be very close to the correct solution for the scheme to work as illustrated in Figure 6. It is found that the exponent 'r' in equation (2.24b) for the initial guess $v^o(x)$ may range from 0.5 to 2.0 but r=1.5 seems to work best in most instances. When there is no solution such as those situations to be discussed later in Section 4.2, the algorithm quickly diverges for a wide range of initial guesses (see Section 3.2 of reference 2 for details). For p-v relations which soften initially and then reharden such as the one studied in Part 2 of this work, the convergence could be very slow and 30-70 iterations may be required depending on the initial guess.

In cases where the algorithm did not converge, the Newton iterative scheme was tried but did not yield convergence either. Per iteration, the Newton scheme takes about 250 times the CPU time needed for Picard's method. For all cases studied Picard's iterative scheme yielded the same results as the Newton method.

4.2. The Characteristics of Admissible p-v Relations.

We examine next how the various characteristics of a given nonlinear p-v relation affect the existence of a solution. This issue is of considerable importance as little is known regarding the fibril p-v behavior that is consistent with observed craze displacement profiles. When 'improper' p-v behaviors are used, the results obtained are necessarily incorrect as discussed in Section 1 concerning recent works in references 28 and 29. (E. Smith [19] and Knauss [22] presented some admissible p-v relations for the crack tip cohesive zone.)

---

13. We tried n=50, 100, 200, 300, 400, 500 and found n=200 to be the best compromise between the integration accuracy (within 0.0001%) and the computing time.

In the present study, we find that there are certain restrictions on the p-v relations for the algorithm to converge. In reference 2, heuristic arguments, similar to the one presented in connection with the finding (1) below, were used to demonstrate that the proposed algorithm is capable of seeking out a solution for a given p-v relation and craze length, if such a solution exists. Otherwise, our numerical studies show it to be most likely that algorithm divergence indicates the absence of a solution. The question of uniqueness is then addressed, but only a brief summary of the findings is included here and the interested reader is encouraged to consult reference 2 for more detail.

Consider the two families of p-v relations depicted in Figure 7.[14] Both models are designed so as to allow the relative amount of hardening and softening in the p-v behavior to be adjusted by varying a few parameters. From the extensive study conducted [2], we draw the following conclusions:[15]

(1) p-v relations with hardening and softening: It is found that only a limited amount of hardening is permissible for a solution to exist.

To demonstrate this finding, consider the following heuristic argument in connection with Figures 8a-e. Assume first that a reasonable craze profile as shown in Figure 8a is the result of prescribing a p-v relation depicted in Figure 8b. Then, without considering continuum mechanics, one deduces from 8a and b the cohesive force distribution in Figure 8c. However, on mechanical grounds i.e. using equation (2.19), this p(x) gives rise to a displacement profile $\tilde{v}(x)$ as shown in Figure 8d which is not equal to that in Figure 8a and exhibits interpenetration in the craze tip region. Moreover, the p-$\tilde{v}$ relation deduced then from

14. Note that in both models, the fibril stress vanishes for displacements greater than a critical value v_c ; we thus deal with a critical crack tip opening displacement (CTOD) criterion which can be justified on physical grounds as is discussed at length in part 2 of this work [1].

15. Quatitative results are given in reference 2.

Figures 8c and 8d and shown in Figure 8e bears little resemblance to the initial p-v relation of Figure 8b. Thus, through this somewhat roundabout argument, we conclude that when the prescribed p-v relation hardens by an 'appreciable' amount prior to softening (as in Figure 8b) and our solution algorithm diverges (i.e. cannot find a solution) for a wide range of initial guesses, there is no solution for the p-v relation prescribed. This line of argument is helpful in ascertaining the nonexistence of a solution when our algorithm fails to produce one.

(2) Monotonically softening p-v relations ($v_m = 0$): We observe that when v_c exceeds certain values, only the trivial solution[16] results, otherwise a nontrivial solution exists. A heuristic argument similar to the one presented in finding (1) above is given in reference 2.

We do not address the question of the uniqueness of solutions rigorously. As is the case in most nonlinear problems, uniqueness is difficult to establish. Nevertheless, based on the extensive experience acquired during the course of this study, we are convinced that for a given craze length and σ_∞, the solution found by using Picard's algorithm is unique. However we find that for a given craze length, there may be two different values of σ_∞ and two corresponding sets of p(x) and v(x) which form solutions: The solution with the higher σ_∞ corresponds to a full craze or a craze with a very short internal crack, while the other one with the lower σ_∞ is invariably the solution of a craze with a 'longer' central crack. These aspects are discussed in more detail in references 1 and 2.

16. The solution corresponding to a fully closed craze, i.e. v(x) = 0 at all points or, simply: No craze exists.

5. CONCLUDING REMARKS

We have shown that the problem of a craze (with or without an internal crack) located in an infinite plane under craze-normal loading can be solved exactly within numerical limitations. The formulation and solution scheme are simple and straightforward. The implemented Picard's algorithm is effective and much more economical than Newton's method. The formulation can also be used, with definite advantage over the presently available schemes, to determine stress distribution profiles and the p-v relations from experimental displacement profiles. Certain characteristics of the fibril force-displacement (p-v) relation which are incompatible with observed craze profiles are pointed out. The methodology developed here is applied in Part 2 of this study [1] in simulating craze and crack growth, yielding an additional set of informative findings.

6. ACKNOWLEDGEMENTS

This work was performed as part of an initiation study into nonlinear crack tip mechanics; it was supported by the Air Force Office of Scientific Research under Grant No. AFOSR-84-0254 with the technical contact being Capt. David Glasgow. Also support from E.I. Dupont de Nemours & Company and NASA under grant NAG-1-474 is gratefully acknowledged. In the past, Drs. K. Palaniswamy and K. Ravi-Chandar have contributed towards the formulation of the problem. We thank Professor E.J. Kramer for the helpful discussions regarding recent experimental findings and for providing us with the micrographs in Figure 1. The first author is also grateful to his colleagues P. Washabaugh and S. Krishnaswamy for their helpful comments and discussions.

7. REFERENCES

1. Ungsuwarungsri, T. and Knauss, W.G., "A Nonlinear Analysis of an Equilibrium Craze, Part II: Simulations of Craze and Crack Growth," Submitted simultaneously for publication, J. Appl. Mech.

2. Ungsuwarungsri, T. and Knauss, W.G., "A Nonlinear Analysis of an Equilibrium Craze in an Infinite Medium Subjected to Symmetrical Loading," GALCIT Report 85-15, California Institute of Technology, Pasadena, CA, 1985.

3. Bucknall, C.B. "Toughened Plastic," Ch. 6, App. Sci. Publ., London, 1977, pp. 136-181.

4. Argon, A.S., Cohen, R.E., Gebizlioglu, O.S., and Schwier, C.E., "Crazing in Block Copolymers and Blends," Advances in Polymer Science, Vol. 52-53, H.H. Kausch (Ed.), Springer-Verlag Berlin, Heidelberg, 1983, pp. 275-334.

5. Kramer, E.J., Advances in Polymer Science, Vol. 52-53 Ch. 1, H.H. Kausch (Ed.), Springer-Verlag Berin, Heidelberg, 1983.

6. Argon, A.S. and Salama, M.M., "Growth of Crazes in Glassy Polymers," Phil. Mag., Vol. 36, 5, 1977, pp. 1217-1234.

7. Lauterwasser, B.D. and Kramer, E.J., "Microscopic Mechanisms of Craze Growth and Fracture," Phil. Mag. A., Vol. 39, 4, 1979, pp. 469-495.

8. Spurr, O.K. and Niegisch, W.D., "Stress Crazing of Some Amorphous Thermoplastics," J. Appl. Polym. Sci., Vol. 6, 23, 1962, pp. 585-599.

9. Kambour, R.P. and Kopp, R.W., "Cyclic Stress-Strain Behavior of the Dry Polycarbonate Craze," J. Polymer Science, A-2, Vol. 7, 1969, pp. 183-200.

10. Hull, D., "The Microstructure and Properties of Crazes," in Deformation and Fracture of High Polymers, Kausch, Hassell, and Jaffe (Eds.) Plenum Press, 1973, pp. 171-189.

11. Kramer, E.J. and Hart, E.W., "Theory of Slow, Steady State Crack Growth in Polymer Glasses," Polymer, Vol. 25, 1984, pp. 1667-1678.

12. Barenblatt, G.I., "The Mathematical Theory of Equilibrium Cracks in Brittle Fracture," in Advances in Applied Mechanics, Vol. VII, Academic Press, New York, 1962, pp. 59-129.

13. Dugdale, D.S., "Yielding of Steel Sheets Containing Slits," J. Mech. Phys. Solids, 1960, Vol. 8, pp. 100-104.

14. Rice, J.R., "Plastic Yielding at Crack Tip," Proceedings of the 1st Int'l Conf. on Fracture, Vol. I, Sendai, Japan, T. Yokobori et al. (Eds.), Japanese Soc. for Strength and Fracture of Materials, Tokyo, 1966, pp. 283-308.

15. Goodier, J.N. and Field, F.A., "Plastic Energy Dissipation in Crack Propagation," Fracture of Solids, D.C. Drucker and J.J. Gilman (Eds.), Wiley (Interscience), New York, 1963, pp. 103-118.

16. Goodier, J.N. and Kanninen, M., "Crack Propagation in a Continuum Model with Nonlinear Atomic Separation Laws," Technical Report No. 165, Div. of Eng. Mech., Stanford University,1966.

17. Atkinson, C. "An Iterative Scheme for Solving Problems Relating to Cracks Opening under a Displacement Dependent Internal Stress," Int. J. Fracture Mech., Vol. 6, 2, 1970, pp. 193-198.

18. Andersson, H. and Bergkvist, H., "Analysis of a Nonlinear Crack Model," J. Mech. Phys. Solids, Vol. 18, 1970, pp. 1-28.

19. Smith, E., "The Structure in the Vicinity of a Crack Tip: A General Theory Based on the Cohesive Zone Model," Eng. Fract. Mech., Vol. 6, 1974, pp. 213-222.

20. Knight, A.C., "Stress Crazing of Transparent Plastics: Computed Stresses at a Nonvoid Craze Mark," J. Polymer Sci, Part A, Vol. 3, 1965, pp. 1845-1857.

21. Sneddon, I.N., Fourier Transforms, McGraw-Hill, New York, 1951, p. 426.

22. Knauss, W.G., "Crack Propagation in Viscoelastic Diaspastically Non-Simple Solids: A Progress Report," Int. Union of Theoretical and Appl. Mech., Mech. of Viscoelastic Media and Bodies Symposium, Gothenburg, Sweden, J. Hult (Ed.), 1974, pp. 263-278.

A more extensive version can be found in Strength and Structure of Solid Materials, a joint Japan-USA seminar, Noordhoff International Publishing, Leyden; H. Miyamoto et al. (Eds.), 1976, pp. 389-416.

23. Verheulpen-Heymans, N. and Bauwens, J.C., "Effect of Stress and Temperature on Dry Craze Growth Kinetics during Low-Stress Creep of Polycarbonate," Part 1 & 2, J. Mat. Sci, Vol. 11, 1976, pp. 1-6 & 7-16.

24. Wang, W.V., and Kramer, E.J., "A Distributed Dislocation Stress Analysis for Crazes and Plastic Zones at Crack Tips," J. Mat. Sci, Vol. 17, 1982, pp. 2013-2026.

25. Donald, A.M. and Kramer, E.J., "The Entanglement Network and Craze Micromechanics in Glassy Polymers," J. Polymer Sci., Polymer Physics Edition, Vol. 20, 1982, pp. 1129-1141.

26. Bevan, L., "Finite Element and Boundary-Element Analysis of Craze Micromechanics," J. Appl. Polymer Sci, Vol. 27, 1982, pp. 4263-4272.

27. Sun, B.N. and Hsiao, C.C., "Nonlinear Quasi-fracture Behavior of Polymers," J. Appl. Phys., Vol. 57(2), 1985, pp. 170-174.

28. Walton, J.R. and Weitsman, Y., "Deformations and Stress Intensities Due to a Craze in an Extended Elastic Material," J. Appl. Mech., Vol. 51, 1, 1984, pp. 84-92.

29. Weitsman, Y., "Nonlinear Analysis of Crazes," J. Appl. Mech., Vol. 53, 1, 1986, pp. 97-102.

30. Tada, H., Paris, P.C., and Irwin, G.R., The Stress Analysis of Cracks Handbook, Del Research Corporation, Hellertown, PA, 1973, p. 5.10.

31. Huang, N.C., "On the Size of the Cohesive Zone at the Crack Tip," J. Appl. Mech. (Brief Notes), Vol. 52, June 1985, pp. 490-492.

8. FIGURE CAPTIONS

Figure 1. Electron micrographs of a craze (a) and its tip region (b). (Courtesy of L. Berger and E.J. Kramer.)

Figure 2. (a) Problem geometry definition
(b) Actual craze contour with primordial craze contour
(c) Linearized geometry: net displacement profile
(d) Model for craze fibril p-v relation

Figure 3. Experimental craze contour from reference 7.

Figure 4. Stress distribution profile derived from V(X) in Figure 3 using the method in Section 3.

Figure 5. The p-v relation derived from Figures 3 and 4.

Figure 6. Convergence illustration v versus x (σ_∞^o = 0.05, r = 1.5). Iterations # 2-8 fall in between iterations # 1 & 9.

Figure 7. Two p-v relations used in studying characteristics of 'admissible'p-v relations.
(a) piecewise-linear model
(b) cosine model

Figure 8. Demonstration of the nonexistence of solution for prescribed p-v relations such as the one in figure (b). See discussion in Section 4.2.

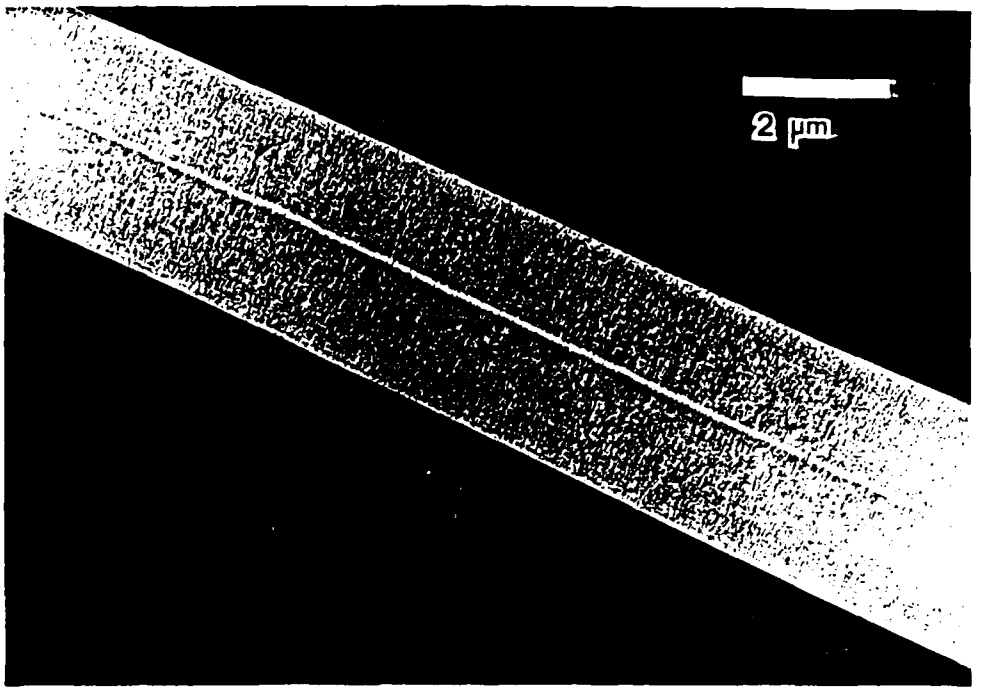

(a)

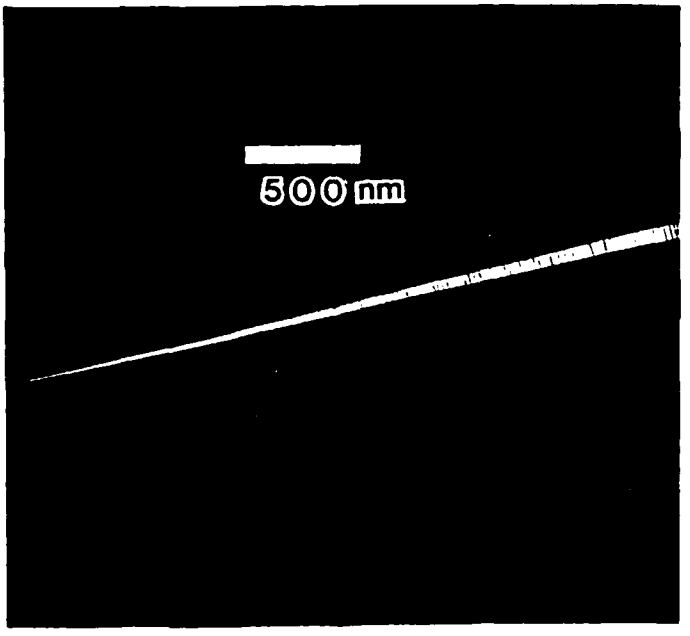

(b)

Figure 1 Electron micrographs of a craze (a) and its tip region (b). (Courtesy of L. Berger and E.J. Kramer.)

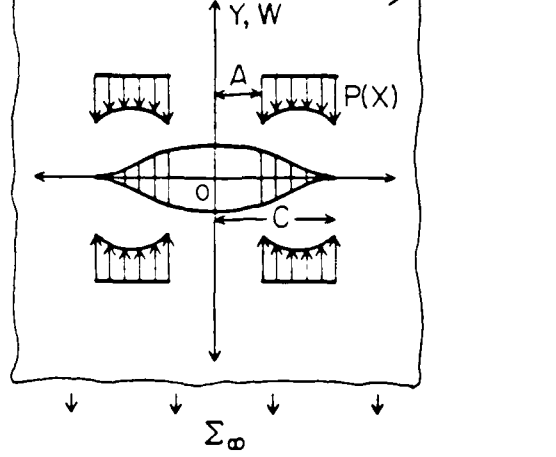

(a)

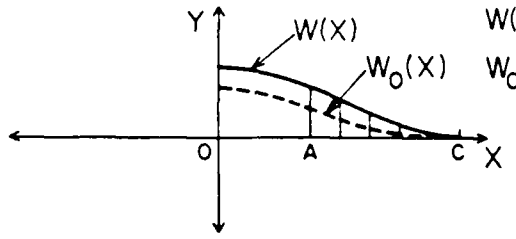

W(X)= Actual craze contour

$W_0(X)$= Primordial craze contour.

(b)

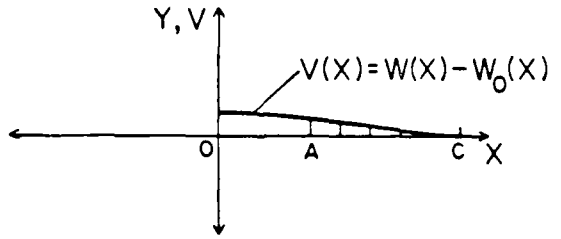

V(X)= Net displacement profile w.r.t. the linearized B.C.'s

(c)

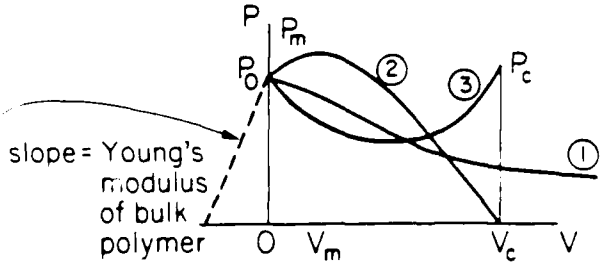

(d)

Figure 2. (a) Problem geometry definition
(b) Actual craze contour with primordial craze contour
(c) Linearized geometry: net displacement profile
(d) Model for craze fibril p-v relation

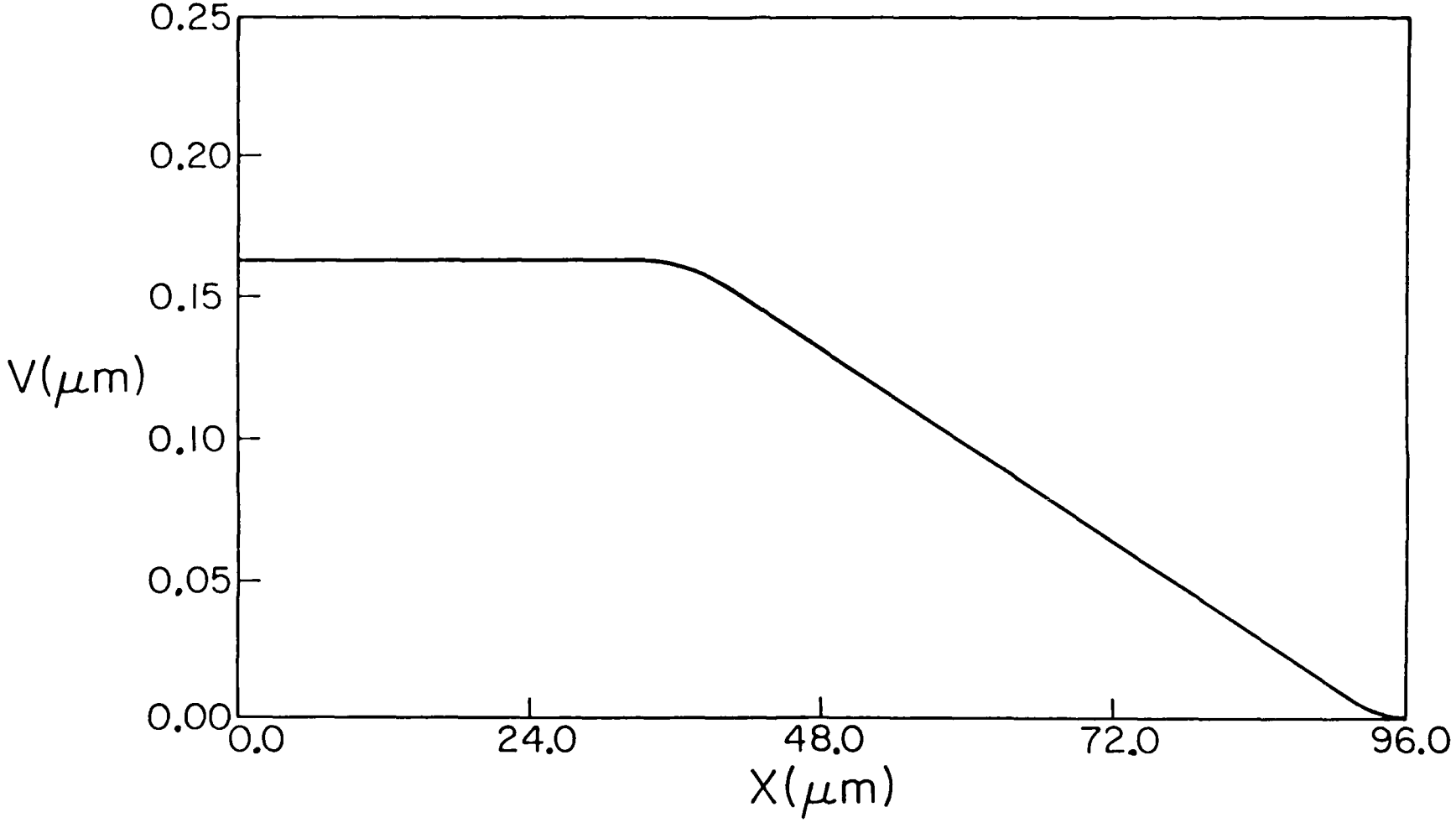

Figure 3. Experimental craze contour from Lauterwasser and Kramer (1979).

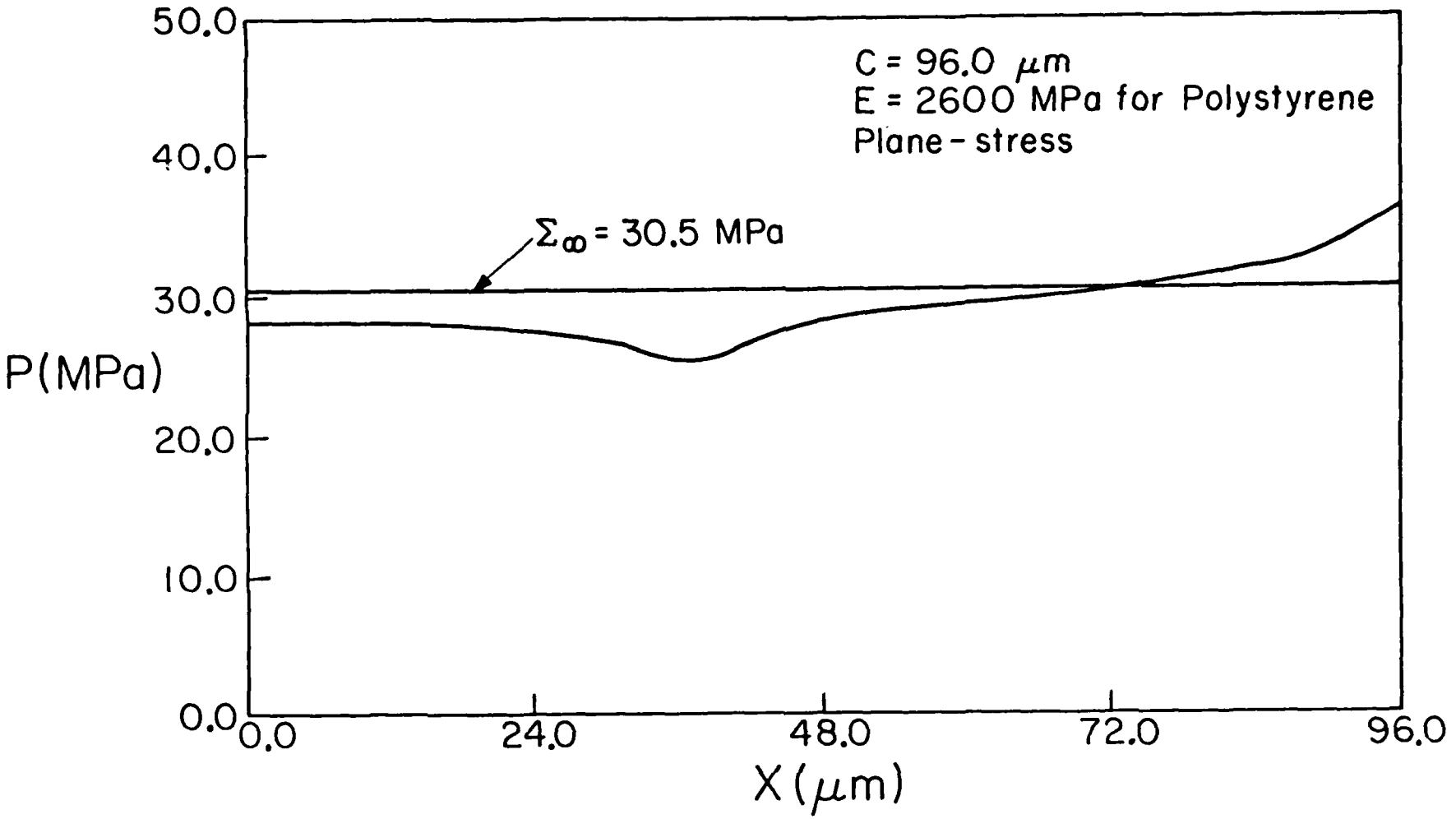

Figure 4. Stress distribution profile derived from V(X) in Figure 3 using the method in Section 3.

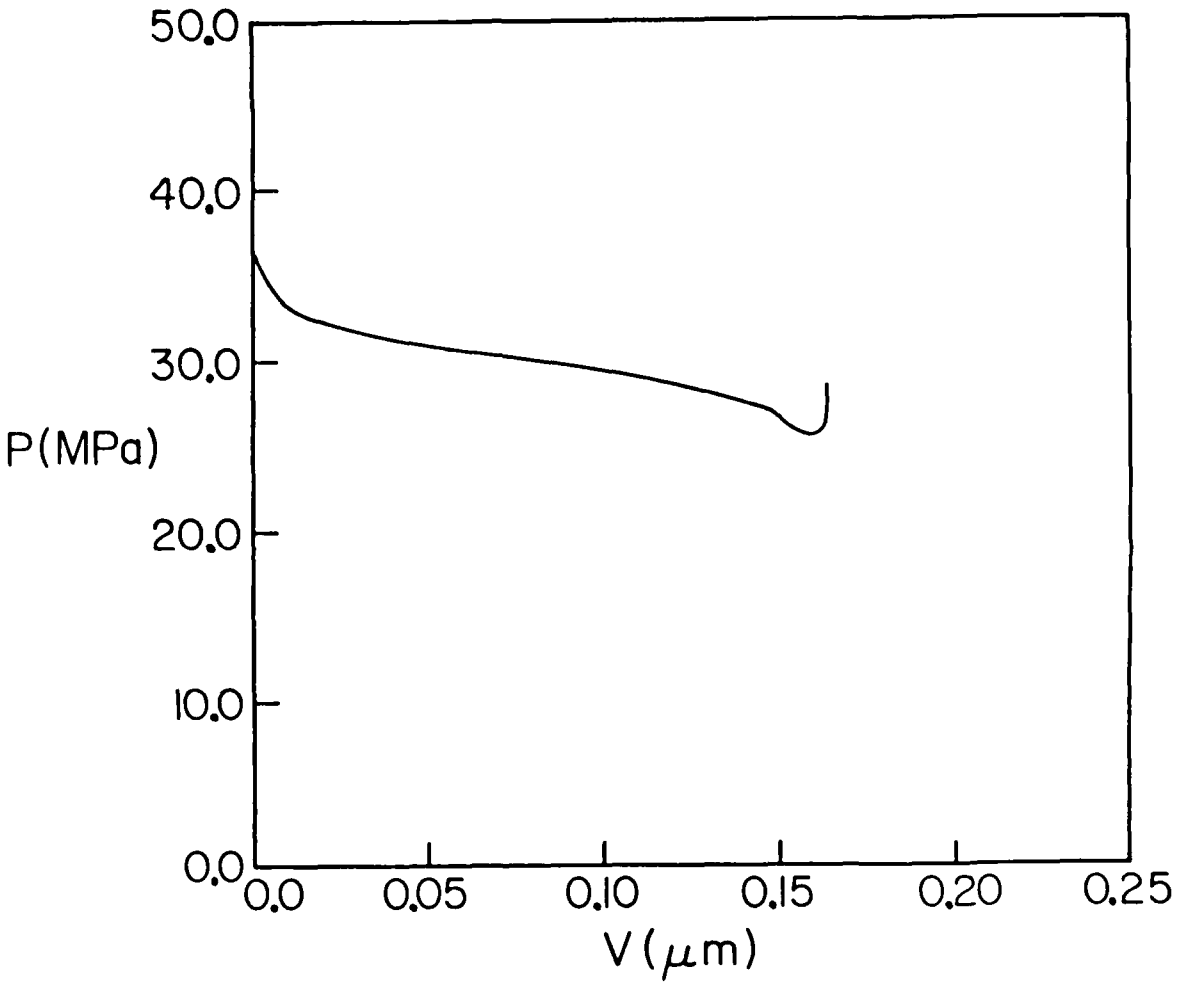

Figure 5. The p-v relation derived from Figures 3 and 4.

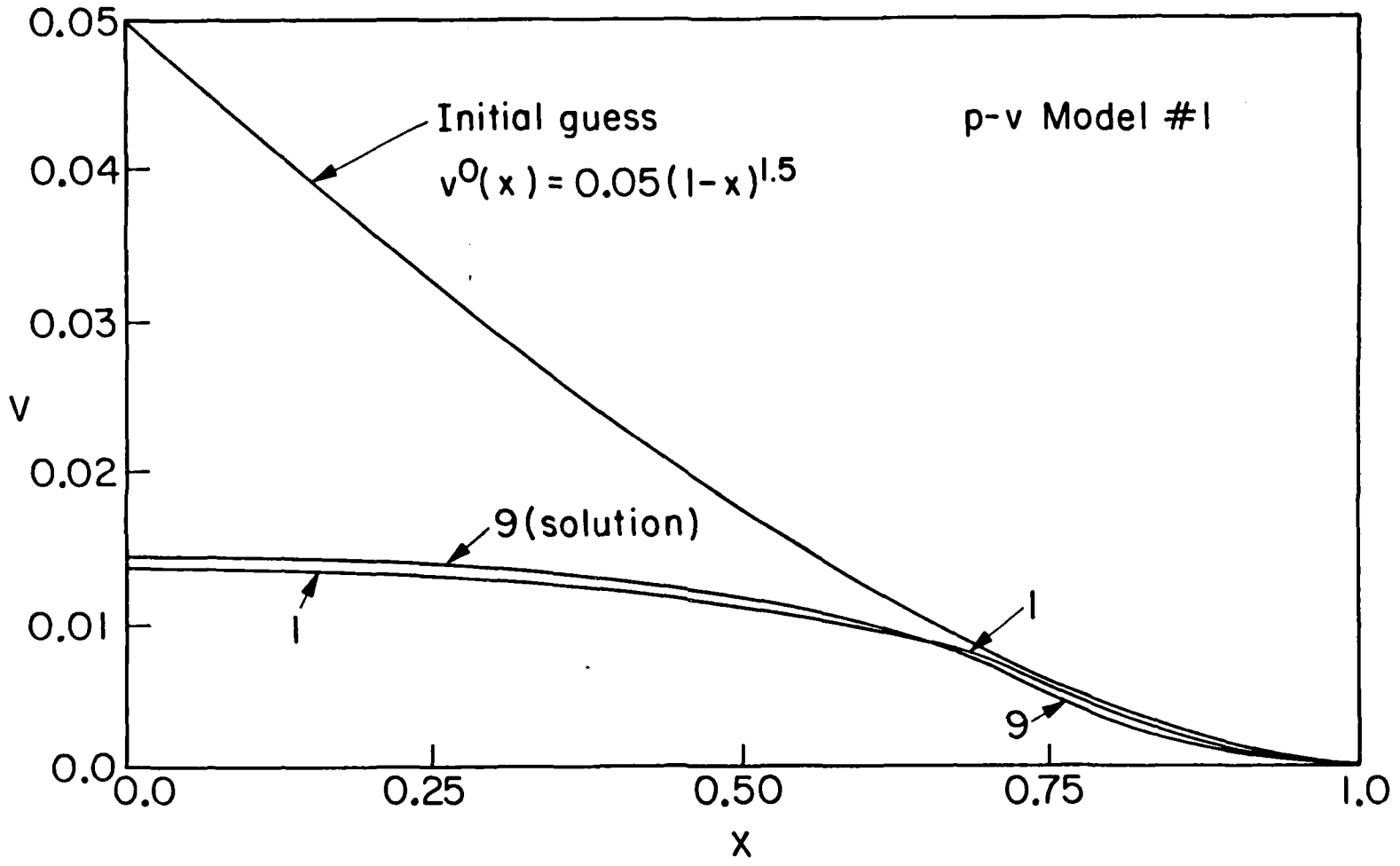

Figure 6. Convergence illustration v versus x ($\sigma_\infty^0 = 0.05$, $r = 1.5$). Iterations # 2-8 fall in between iterations # 1 & 9.

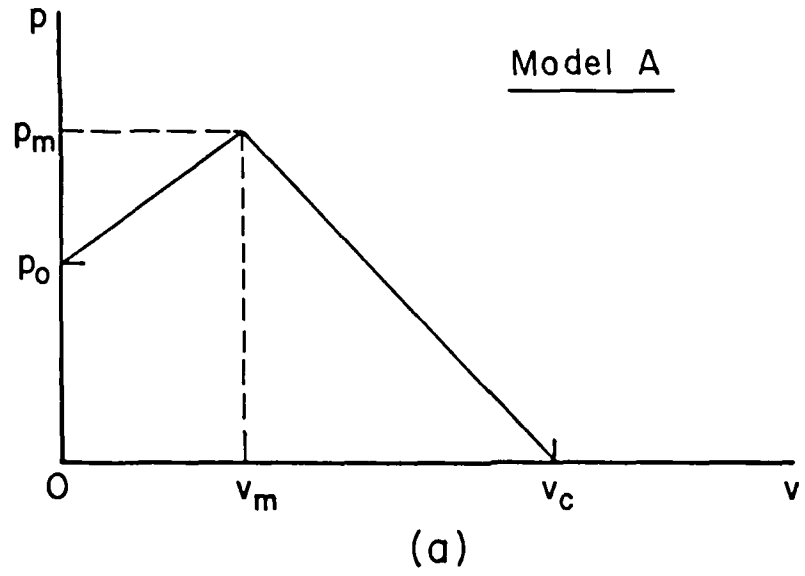

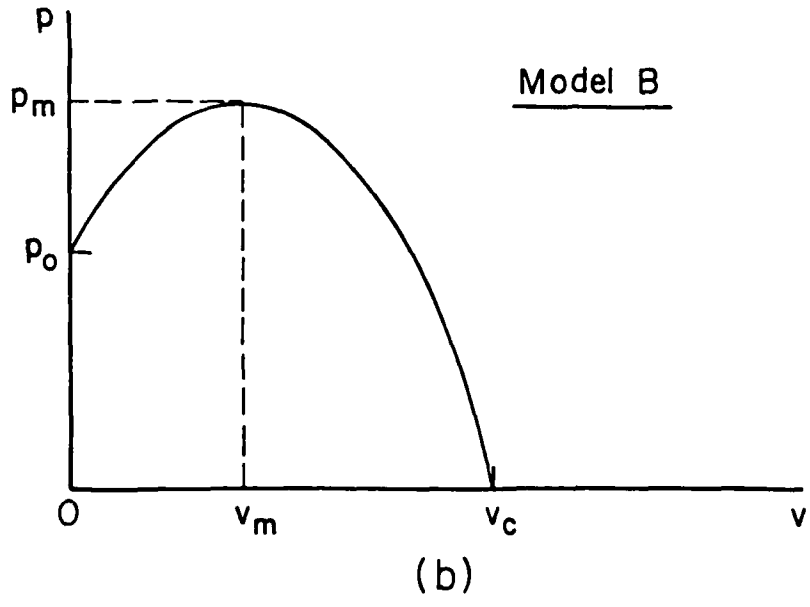

Figure 7. Two p-v relations used in studying characteristics of 'admissible'p-v relations.
(a) piecewise-linear model
(b) cosine model

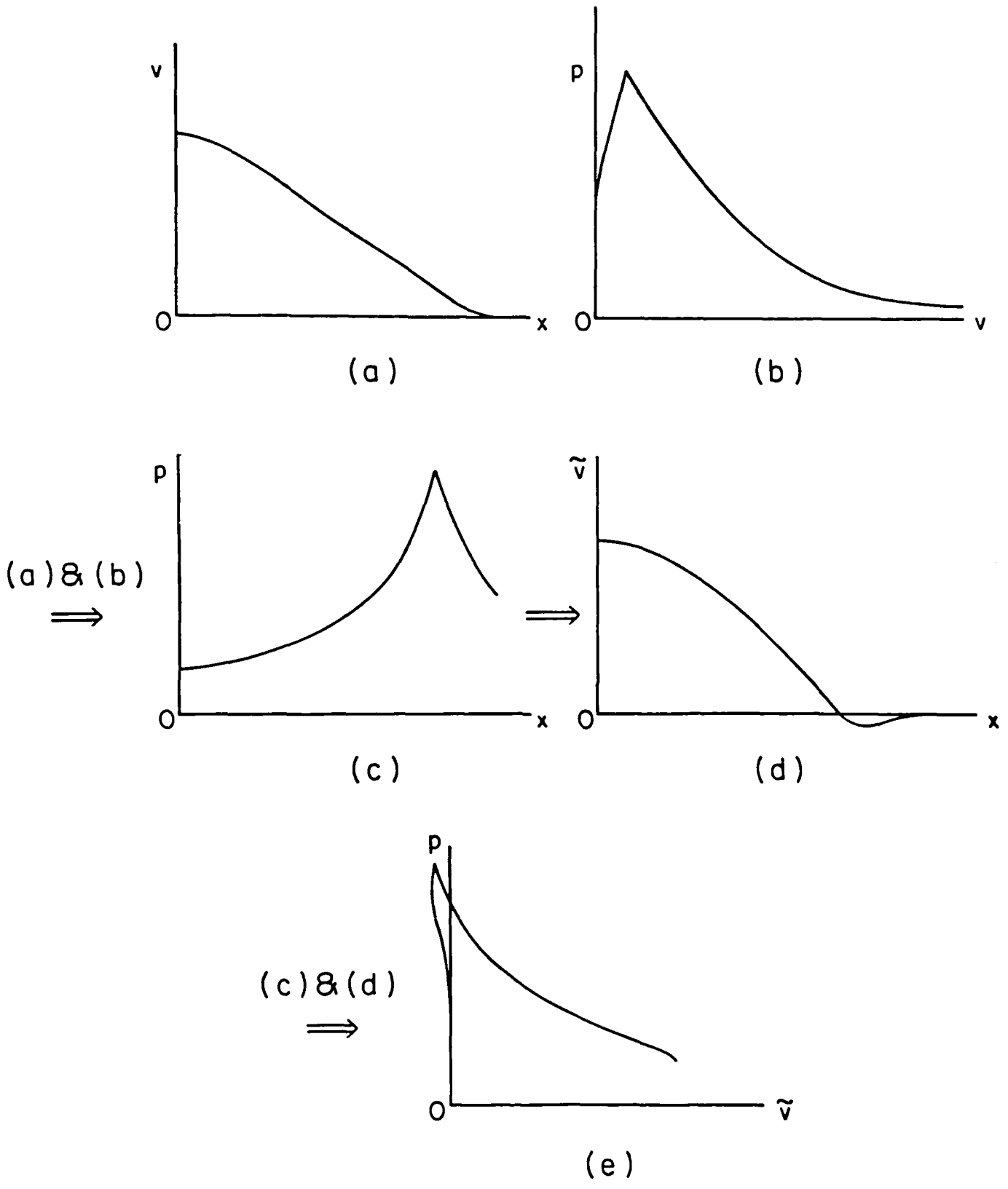

Figure 8. Demonstration of the nonexistence of solution for prescribed p-v relations such as the one in figure (b). See discussion in Section 4.2.

SM 85-15-2

A NONLINEAR ANALYSIS OF AN EQUILIBRIUM CRAZE
PART II: SIMULATIONS OF CRAZE AND CRACK GROWTH

by

T. Ungsuwarungsri* and W.G. Knauss**

Graduate Aeronautical Laboratories
California Institute of Technology
Pasadena, CA 91125

---

* Graduate Research Assistant

** Professor of Aeronautics and Applied Mechanics

ABSTRACT

In this study we investigate the effects of nonlinear fibril behavior on the mechanics of craze and crack growth. The effect of strain-softening cohesive material on crack stability is of particular interest and is examined via a craze and crack model developed in reference 1 where the formulation and solution of the problem are discussed.[1]

In this second part, quasi-static growth of a craze with a central crack is analyzed for different nonlinear force-displacement (p-v) relations for the craze fibrils. A 'critical crack tip opening displacement' (CTOD) or more precisely, 'critical fibril extension' is employed as the criterion for fracture. The p-v relation is further assumed to be invariant with respect to the craze and crack lengths. The results are compared with the Dugdale model; the craze zone size and the energy dissipation rate approach asymptotic values in the limit of long cracks.

The problem of craze growth from a precut crack under increasing far-field loading is then studied. In the case where the p-v relation is monotonically softening, the crack can start to grow in an unstable manner before the crack tip opening displacement reaches its critical value.

1. Here all quantities are presented in their nondimensionalized forms as defined in reference 1. The unabridged version of this work is given in reference 2.

1. INTRODUCTION

In reference 1 the mathematical and experimental treatment of craze formation were summarized. We developed there an analytical and computationally efficient scheme to obtain the stress distribution and displacement profiles of a craze/crack for a prescribed craze length and an arbitrarily nonlinear force-displacement (p-v) behavior of the craze fibrils. The solution scheme developed in references 1 and 2 is here applied to investigate how the nonlinear fibril p-v characteristics affect the mechanics of craze and crack growth. The critical crack tip opening displacement (CTOD) is employed in a natural way as a fracture criterion. The applicability of this CTOD criterion to crazes containing cracks is based on experimental evidence and will be discussed in the next section. It is assumed that under quasi-static conditions the fibril p-v relation does not change its character as the craze and crack propagate. This assumption is made for lack of experimental data and because of an inadequate understanding of the fibril behavior at the present time. In a later section, we examine the problem of a craze initiating from an existing (precut) crack with special interest on the effect of 'softening' fibril behavior on crack stability.

2. THE TWO BASIC ASSUMPTIONS

We examine first the 'crack tip opening displacement' criterion (CTOD) and the 'invariance' assumption regarding the fibril p-v behavior as the craze and crack grow in the light of existing experimental results. Of these separate issues we address first

2.1. The CTOD Criterion.

When a central crack is present within a craze, the crack may or may not propagate as the far-field load σ_∞ is increased. If the crack does not propagate, it is clear that the fibril at the crack tip can sustain

additional growth (lengthening) though not necessarily higher stress or strain. This is the consequence of two physical mechanisms that operate simultaneously, namely, surface drawing and fibril creep.[2] If surface drawing alone operates, a fibril will never break and the crack will never advance. This possibility is contrary to experimental observations since cracks do grow within crazes. As can be explained in terms of craze and fibril microstructures, a crack that propagates quasi-statically through a craze either runs right along the midrib where the fibrils are weakest or propagates in a 'patch' or 'mackerel' pattern [3,4]. In the first situation, the heightened stress at the crack tip causes the previously unloaded midrib to stretch until the local extension ratio exceeds the maximum sustainable by the bundles of polymeric molecule chains that constitute the fibril, thus leading to fracture. In the latter event, usually observed at higher crack velocities [4], the high crack tip stress causes fibrils at the craze-polymer interface to be drawn at high local strains [3]. One observes then that the crack, in this case, prefers to run along either interface where the fibrils are locally weaker than at the midrib, creating the familiar mackerel pattern [3,4]. In either case, the above situations support the use of a critical crack tip opening displacement (or a critical fibril extension criterion). This is also confirmed by experiments performed by Döll et al [5,6] who found that the CTOD is relatively constant for a wide range of crack velocities. Specifically, these authors showed that the maximum craze widths at the crack tip (critical CTOD or v_c in our notation), measured in PMMA compact tension specimens for crack speeds ranging from 10^{-8} to 20 mm/sec, are essentially constant with a standard deviation of about 8%.[3] Their findings

2. Surface drawing is the process by which bulk polymer is converted (drawn) into fibrillar craze material. Fibril creep is simply the stretching of an existing fibril without drawing additional polymer material into the craze from the bulk.

3. In private communication, Professor Kramer indicated that under a low crack speed of about 1 micron/sec the critical CTOD increases substantially. This casts some doubt on the validity of the number 10^{-8} mm/sec given in references 5 and 6. However, for the speed range between 10^{-3} and 20 mm/sec, the constancy of the CTOD (for PMMA) appears acceptable. See the introduction of reference 13 for further discussion on this point.

suggest that the fibrils spanning the tip of the crack can only sustain a limited, relative, displacement of their ends. An interpretation of the experimental result in terms of molecular behavior is given in reference 6; such discussions are beyond the scope of the present work. For our purpose, it suffices to assume that the surface drawing mechanism is somehow constrained at the crack tip and creep invariably gives rise to fibril breakage at a roughly constant CTOD.[4] We assume in this study, therefore, that for a given polymer, a critical CTOD exists and is constant.

2.2. Comments on the Invariance of the p-v Relation.

To study craze and/or crack growth, one needs to know whether the p-v relation changes as propagation proceeds and if so, how. The question can only be answered by experiments. Since no experimental data on this particular topic is available, we feel free to assume further that the p-v relation is 'invariant' with respect to both the craze and the crack lengths for quasi-static propagation under a 'controlled' environment.[5] As it turns out, on the basis of the subsequent studies, this assumption can only be valid over a limited range of craze and crack lengths (see Section 3).

3. NUMERICAL SIMULATIONS OF CRAZE AND CRACK PROPAGATION

We proceed now to apply the solution scheme of reference 1 to study how the nonlinear fibril (cohesive) p-v characteristics affect the mechanics of craze and crack growth. The geometry of the problem [6] is depicted

---

4. It is worthwhile to note that cracks are observed to form in 'full' crazes at the polymer/craze interface and not at the midrib. The locations of the first formed crack in a full craze are also not necessarily at the center part of the craze where the fibrils are longest.

5. Temperature, pressure, moisture content, chemical environment (such as the presence of alcohol or any chemical agents possibly affecting fibril drawing and creep) are all kept unchanged.

in Figure 1: The craze length is denoted by c, the crack length by 'a' and the vertical boundary displacement of the craze by v. The remotely applied stress is σ_∞ and the fibril cohesive force is represented by p.[7] Given a craze length and a p-v relation for the fibrils, the problem is to find p(x),v(x) and σ_∞ such that both equilibrium and the smooth closure (Barenblatt's) condition are satisfied simultaneously.[8] The solution scheme is presented in references 1 and 2.

Quasi-static craze and crack growth is simulated by varying the craze length c continuously. Based on the discussion in Section 2, we assume the fibril force-displacement relation of the form

$$p(x) = p[v(x)] \tag{3.1}$$

The effect of several p-v relations will be examined. We start by first reviewing the Barenblatt-Dugdale model [7,8] shown in Figure 2.

3.1. The Barenblatt-Dugdale Model.

This simplest model assumes constant cohesive (fibril) stress throughout the cohesive (craze) zone as denoted by p_m in Figure 2. The problem has been analyzed by Rice [9] and Goodier and Field [10]; we summarize below the pertinent results for reference.[9] They are obtained directly from the equations presented in Section 2 of reference 1. The

---

6. We consider here the planar problem i.e. plane stress or plane strain.

7. The mathematical modelling of the problem has been described in references 1 and 2.

8. In this paper, the (net) stress intensity factor is always zero and thus does not enter the discussion as a pertinent parameter. The external loading is completely characterized by σ_∞ which is related to the 'loading' stress intensity factor by $K_I = \sigma_\infty \sqrt{\pi c}$. Note that the stress states at both the crack tip and the craze tip are determined by the nonlinearity of the fibril p-v relation rather than the 'usual' K-field.

9. All equations and parameters are in dimensionless forms.

Barenblatt condition requires

$$\sigma_\infty = \frac{2}{\pi}\, p_m \cos^{-1}\left(\frac{a}{c}\right) \tag{3.2}$$

and the displacement v(x) is

$$v(x) = \frac{p_m}{\pi}\left[a\log\left| \frac{\sqrt{c^2-x^2}+\sqrt{c^2-a^2}}{\sqrt{c^2-x^2}-\sqrt{c^2-a^2}} \right| + x\log\left| \frac{x\sqrt{c^2-a^2}-a\sqrt{c^2-x^2}}{x\sqrt{c^2-a^2}+a\sqrt{c^2-x^2}} \right| \right] \tag{3.3}$$

At x=a, v equals v_c the critical CTOD, thus applying L'Hospital's rule, one obtains

$$v(a) = v_c = \frac{2p_m}{\pi}\, a\, \log\left(\frac{c}{a}\right) \tag{3.4}$$

Let ω denote the size of the craze (yield) zone, i.e.

$$\omega \equiv c - a \tag{3.5}$$

Further, let γ be the 'fibril fracture energy' (or the 'surface energy') which is the work expended in pulling a fibril from v = 0 to $v = v_c$. For the Barenblatt-Dugdale model, we have simply

$$\gamma \equiv p_m v_c \tag{3.6}$$

By analyzing the data for six polymers in references 3 and 11, we find that the dimensionless parameters p_m and v_c have values in the ranges of

$$0.01 \leq p_m \leq 0.1$$

$$0.001 \leq v_c \leq 0.01$$

We shall use these numbers later as guides for bounding the various parameters in the p-v relations to be studied so that the results of our

analyses will be quantitatively meaningful.

We examine next the energy release rate of the system. Let U represent the elastic energy of the system. The energy release rate G is defined as in terms of the potential energy Π as

$$G = - \frac{\partial \Pi}{\partial a} \tag{3.7}$$

Consider the fixed grip case so that no external work is done during the course of crack propagation. Then (3.7) reduces to

$$G = - \frac{\partial U}{\partial a} \tag{3.8}$$

Now U is given by the elastic energy stored initially in the plate (planar body), U_p, minus the energy U_c which is required to form a crack of length 2a and two craze zones of length ω each. We have then

$$U = U_p - U_c \tag{3.9}$$

$$U_p = \frac{1}{4} \sigma_\infty^2 d^2 \tag{3.10}$$

where we let d denote the dimension of this 'infinite' square plate (i.e. $d >> c$).[10] U_c is given by

$$U_c = 4 \left[\gamma a + \int_a^c p_m v(x) dx \right] \tag{3.11}$$

where the factor of 4 accounts for the four quadrants. Substituting v(x) from (3.3) and making use of (3.2) and (3.4), one obtains after some algebra

10. Note that the factor 1/4 in place of the normally expected factor of 1/2 is a result of the particular non-dimensionalization scheme employed.

$$U_c = 4a[\ \gamma + \frac{p_m}{2}\ (\ \sigma_\infty \sqrt{c^2-a^2} - 2v_c\ )\ ] \tag{3.12}$$

Using (3.9) and (3.10) in (3.8) yields

$$G = -\frac{1}{2}\ \sigma_\infty d^2\ (\ \frac{\partial \sigma_\infty}{\partial a}\ ) + \frac{\partial U_c}{\partial a} \tag{3.13}$$

At this point an important question enters: What is the criterion for crack propagation (fracture) ?

Goodier and Field [10] assumed that the crack grows in a self-similar manner, such that

$$\frac{\partial c}{\partial a} = \frac{c}{a} \tag{3.14}$$

This condition is the consequence of assuming σ_∞ to be constant as the crack and craze grows. Under these conditions, $\frac{\partial \sigma_\infty}{\partial a}$ vanishes and G becomes, in view of (3.13), $\frac{\partial U_c}{\partial a}$, which is the 'plastic' (cohesive) work rate. However, the crack tip opening displacement $v(a) = v_c$ as given by (3.4) becomes a linear function of a. Thus the CTOD in the model presented by Goodier and Field model increases as the crack grows. This behavior is inconsistent with experimental observations as discussed in Section 2.

In the present model, the critical CTOD, v_c, is kept constant; this condition in turn requires that σ_∞ must decrease as 'a' increases (see Figure 7) in order to maintain the quasi-static condition, i.e.

$$\frac{\partial \sigma_\infty}{\partial a}\ |_{v_c} < 0 \tag{3.15}$$

Viewing (3.13) in this light, it is evident that G becomes unbounded if d is unbounded, no matter how small $\sigma_\infty(\frac{\partial \sigma_\infty}{\partial a})$ may be, since $\frac{\partial U_c}{\partial a}$ is always fin-

ite.

Therefore, a crack, the tip displacement of which has reached the critical value, is always unstable in this geometry.[11] To this result we only need to add the reminder that for a clamped infinite (very large) plate, a small enlargement of an internal crack would hardly reduce the far-field σ_∞ sufficiently to keep the crack and craze growing in a quasi-static manner. Therefore once a crack (with or without a cohesive zone) starts growing, and the fracture criterion such as a critical CTOD is satisfied, catastrophic failure ensues. We shall see later that the converse is not true.

The plastic work rate, $\frac{\partial U_c}{\partial a}$, calculated using the CTOD criterion differs markedly from the result obtained by Goodier and Field under the assumption of self-similar growth (see [2] and [10] for details). Based on the present criterion, the plastic work rate increases as 'a' increases and approaches the constant value 4γ rapidly. Physically, for a short crack, one has a relatively large craze zone ω ; to advance the crack by an amount Δa, very little energy is needed since c increases more slowly than 'a' (i.e. the craze zone ω shrinks). For longer cracks, the size of the craze zone tends toward a constant value and thus the craze zone simply translates as the crack propagates. In this latter case, the dissipated energy is thus 4γ per unit crack advance. This is demonstrated later in Figure 8 together with results for other nonlinear p-v models.

3.2. General p-v Models.

Next we examine six different p-v relations labeled #1 through #6 in Figure 3 and compare the results to the Dugdale model labeled 'D'. Model #6 approximates the p-v behavior of craze fibrils as it is known today

11. If the tip displacement is less than v_c, the crack does not grow as the tip fibril has not yet been broken. For softening p-v relations, however, instability may occur before v_c is reached (see Section 4).

[11,12]. As a check, we employ this model to simulate craze and crack growth. The resulting craze contours and stress distribution profiles are depicted in Figures 4 and 5 respectively. They do closely resemble the experimental v(x) and p(x) obtained by Kramer and his coworkers [11,12].

To compare the results for all these different p-v relations, it is desirable to use the Dugdale model as a benchmark (here we use the model labeled 'D' in Figure 3 with $p_m = 0.025$ and $v_c = 0.008$). All the p-v models are designed so that the area under each p-v curve, γ , is constant and equal 2×10^{-4}, the same as that for the Dugdale model employed.

The numerical procedures have been presented in Section 2.3 of reference 1. The craze length is varied from c = 0.0 to c = 10.0, the increment Δc ranges from 0.01 to 0.2. Smaller increments for Δc are necessary to capture the behavior of the system for short crack lengths, particularly in calculating the rate of plastic work, $\frac{\partial U_c}{\partial a}$.[12] During the course of these craze growth simulations, it was found that convergence is generally attained in fewer iterations if $v_i(c)$ is used as the initial guess of $v_i(c+\Delta c)$. (This is not the case for p-v model #6, however.) In order not to confuse the presentation of the results, the trivial solution which occurs at short craze lengths and corresponds to a closed craze (v(x) = 0) is not included. Also, for the Barenblatt-Dugdale model 'D', results that are 'nonphysical' in the sense of a crack growing in a shrinking craze, are omitted. Interested readers are refered to reference 2 for more details.

In Figure 6, the craze zone ω is plotted as a function of the crack length 'a'. The craze zone is seen to decrease monotonically and to tend toward constant asymptotic values as 'a' increases for all p-v models.[13]

---

12. U_c is obtained by integrating numerically

$$U_c = 4\left[\gamma a + \int_a^c ev(v(x))dx\right] \qquad \text{where} \qquad ev(v) = \int_o^v p(v')dv'$$

13. For the Barenblatt-Dugdale model, this can be analytically shown to be the case.

Thus in the limit of long cracks, the craze zone is simply shifted as the crack and craze grow. Note that ω is primarily dependent on v_c but also depends weakly on the character of the p-v relation.

In Figure 7, the far-field stress σ_∞ normalized by $p_m = 0.025$ is plotted versus c for the various p-v models. The remotely applied stress decreases monotonically as the craze/crack grows which is necessary to maintain quasi-static growth. This confirms the conclusion reached in the previous section from the energy release rate analysis that once the critical CTOD is reached the crack will grow unstably if the remotely applied stress is maintained constant. An interesting feature is exhibited by the dash-dot curve which represents a 'full craze' (a = 0) solution branch and is present only in the p-v model #6 (among all models studied here). This unusual behavior merits further elaboration:

One finds that for a craze length $c < 0.8$, the algorithm converges to the trivial solution in which the craze is closed ($v(x)=0$) at all points (see Figure 13). For c greater than 0.8, there exists a 'full craze' solution regime up to $c = 2.2$. At $c = 2.2$, the solution shows that $v(o)$ is approximately 0.006 and thus $p(x)$ has a minimum at $v(x) = 0.005$ (see Figure 3). For c larger than 2.2, there is no full craze solution (the algorithm 'jumps' and converges to solutions with cracks i.e. $a \neq 0$). This behavior can again be explained using a heuristic argument, see Section 3.2 of reference 2. Note that for $1.87 < c < 2.2$, the solutions are not unique, i.e. for a given c in this range, we either have a full craze solution at a higher σ_∞ or a crack/craze solution at a lower σ_∞.

The above result, which indicates the absence of solutions for the prescribed p-v relation (#6) over some ranges of craze and/or crack lengths may seem, at first sight, contradictory to our physical intuition: One would think that crazes and/or cracks of different sizes should exist in a continuous size 'spectrum'. This seeming contradiction is resolved by recognizing that, most probably, the p-v relation is not 'invariant' with respect to all values of the crack and craze lengths as initially

assumed.[14] More elaborate modelling of the fibril p-v characteristic is therefore needed; see Section 5 for further discussion.

In Figure 8, the rate of 'plastic' work, $\frac{\partial U_c}{\partial a}$, is plotted as a function of the crack length 'a'. It approaches the asymptotic limit 4γ fairly quickly for all p-v models studied.[15]

4. CRAZE GROWTH INITIATING FROM A PRECUT CRACK

In this section, we consider the problem of a craze growing from a precut slit as shown in Figure 9. Under the assumption of a CTOD criterion, one would expect the crack to start advancing when the remotely applied stress σ_∞ is high enough to make the crack tip displacement v(a) reach the value v_c. Thereafter the crack and craze would grow unstably as discussed in the previous section.

However, it is conceivable that for certain p-v relations, σ_∞ may reach its maximum value before the crack tip opening displacement reaches its critical value v_c , thus resulting in instability before the CTOD criterion is satisfied. We shall show that this is indeed the case for p-v relations that soften monotonically up to fracture (fibril breakage). To start, let us first study the Barenblatt-Dugdale model for later reference.

---

14. Note that this conclusion is based solely on mechanics analysis.

15. The curve representing p-v model #6 has been smoothed out for $a > 2.5$. For this particular p-v relation, to get accurate v_c in the craze zone (whose size is = 0.8 for $a > 2.5$), finer discretization is required to capture the steep rise and fall of the stress distribution in the craze zone.

4.1. The Barenblatt-Dugdale Model.

We start with a precut crack of length $2a_o$. Initially the craze length $c = a_o$, i.e., $\omega = 0$. We then increase σ_∞ gradually until v(a) reaches v_c. By equation (3.4) when $v(a) = v_c$, the 'critical' craze length c_{cr} is

$$c_{cr} = a_o \exp \frac{\pi v_c}{2p_m a_o} \tag{4.1}$$

Hence for $a_o \leq c < c_{cr}$, the remotely applied stress σ_∞ can be obtained from (3.2), i.e.

$$\sigma_\infty = \frac{2p_m}{\pi} \cos^{-1}\left(\frac{a_o}{c}\right), \qquad a_o \leq c < c_{cr} \tag{4.2}$$

Based on (4.1) and (4.2), we can plot the applied stress σ_∞ as a function of c for constant $a = a_o$ as shown in Figure 10. Four initial crack lengths are used (a_o= 0.6, 0.9, 1.2, and 1.5). The curve representing quasi-static crack and craze growth referred to subsequently as the 'master' curve) and on which the CTOD always attains its critical value is also identified. On the 'master' curve, the craze and crack growth is unstable in the sense that σ_∞ must be reduced continually in order to maintain quasi-static propagation.

Along the curves on which $a = a_o$, the CTOD v(a) gradually grows as the remotely applied stress σ_∞ is increased e.g. from point A to B; it then reaches its critical value v_c at B. Thus for the Barenblatt-Dugdale model, σ_∞ increases monotonically in the process and instability can occur only when the 'master' curve is reached.

4.2. General p-v Models.

Next let us consider the same problem as in Section (4.1) using p-v relations #1 through #6 of Figure 3. In contrast to the Barenblatt-Dugdale model, we find that for p-v relations that soften monotonically up to the point of fracture (models #1 through #5) instability may occur before the critical CTOD is reached at the crack tip. Briefly, the numerical analysis proceeds in the following sequence:

i. Start with a value a_o which corresponds to a c_{cr} that lies on the master curve.

ii. Increase c gradually from a_o to c_{cr} in such way that the crack tip falls exactly on a discretized point x_i . This avoids unnecessary interpolation.

iii. Find the solution, pre-specifying that p(x) vanish for $x \leq a_o$. The solution would automatically have $v(a) < v_c$ as long as $c < c_{cr}$.

For illustrative purposes we present first the result for model #5 as being representative of the class of monotonically 'softening' p-v models (#1 through #5). More complete results are given in [2]. In Figures 11 and 12 (enlargement of a part of Figure 11), one sees that, for $a_o = 0.3$ to 1.5, instabilities occur before the 'master' curve is reached.

Consider a stress-controlled experiment. As the far-field stress σ_∞ is increased from zero to point B (Figure 12), the CTOD, i.e. v(a), approaches the critical CTOD, v_c. At B, any further increase in σ_∞ will cause the crack and craze to grow unstably since quasi-static growth will no longer be maintained at that stress level. If one reduces σ_∞ instead, keeping in mind that the craze length c cannot decrease while $a = a_o$ remains constant, point C could then be reached quasi-statically. Therefore, at point B, any small positive perturbation in σ_∞ or in a_o would cause the crack and craze to grow in an unstable manner. Note that the

solution cannot 'jump' spontaneously from point A to point C because more work has to be done to further develop to the craze zone and this is achieved by following the path ABC as discussed.

To explore this instability further, consider perturbing the system at point A by cutting fibrils at the crack tip making a_o increase infinitesimally. Does this cause catastrophic failure? As depicted in Figure 12, the solution will then move from point A to a nearby point D which corresponds to $a_o = 0.3^+$ and stop. Thus the craze and crack at point A is stable since a small perturbation in a_o does not lead to total failure. Note in passing that the unstable behavior is more pronounced for the shorter initial crack lengths.

We turn next to the result for p-v model #6 which rehardens after the initial softening and fails abruptly as in the Barenblatt-Dugdale model (see Figure 13). One sees that the unstable character observed in softening p-v models is clearly absent which closely resembles the result for the Barenblatt-Dugdale model shown in Figure 10. These results indicate that in cases where craze fibrils fail in an abrupt manner (as opposed to gradual softening to rupture), instability does not take place until the CTOD reaches its critical value v_c.

5. CONCLUDING REMARKS

In this second part of the study, we have examined the quasi-static growth of cracks and crazes by considering a number of nonlinear fibril p-v models along with the Barenblatt-Dugdale model. The energy dissipation rate consistent with the critical CTOD criterion is established for these materials. We also considered the case of craze growth starting from a precut crack; under these circumstances instabilities are observed to occur before the critical CTOD is reached at the crack tip for p-v models that soften monotonically to fracture.

As discussed earlier, not enough is known about the p-v characteristics of the craze fibrils. Further investigation into the interplay between the surface drawing and creep mechanics should shed some light on how the p-v behavior of fibrils changes as the craze and crack grow; a first attempt along this line has been undertaken by Kramer and Hart [13]. Experiments such as those performed by Kramer et al. [3,11,12] need to be carried out for a wider range of craze and crack lengths to determine to what extent the fibril p-v relation is invariant with respect to c and 'a'.

6. ACKNOWLEDGEMENTS

This work was performed as part of an initiation study into nonlinear crack tip mechanics; it was supported by the Air Force Office of Scientific Research under Grant No. AFOSR-84-0254 with the technical contact being Capt. David Glasgow. Also support from E.I. Dupont de Nemours & Company and NASA under grant NAG-1-474 is gratefully acknowledged. We thank Professor E.J. Kramer for the helpful discussions on the physical aspects of the problem. The first author is also grateful to his colleagues; Mr. Washabaugh and Mr. Krishnaswamy for their many helpful comments and discussions.

7. REFERENCES

1. Ungsuwarungsri, T. and Knauss, W.G. "A Nonlinear Analysis of an Equilibrium Craze, Part I: Problem Formulations and Solutions," Submitted simultaneously for publication, J. Appl. Mech.

2. Ungsuwarungsri, T., and Knauss, W.G., "A Nonlinear Analysis of an Equilibrium Craze in an Infinite Medium Subjected to Symmetrical Loading," GALCIT Report 85-15, California Institute of Technology, Pasadena, CA, 1985.

3. Lauterwasser, B.D. and Kramer, E.J., "Microscopic Mechanisms of Craze Growth and Fracture," Phil. Mag. A., Vol. 39, 4, 1979, pp. 469-495.

4. Hull, D., "The Microstructure and Properties of Crazes," in Deformation and Fracture of High Polymers, Kausch, Hassell, and Jaffe (Eds.) Plenum Press, 1973, pp. 171-189.

5. Schinker, M.G. and Döll, W., "Interference Optical Measurements of Large Deformations at the Tip of a Running Crack in a Glassy Thermoplastic," Physics Conference Series No. 47, J. Harding (Ed.), Inst. of Physics, Bristol, England, 1979, pp. 224-232.

6. Döll, W., Schinker, M.G. and Koenczoel, L., "A Time Independent Fracture Criterion for PMMA ?," Int. J. Fracture, Vol. 15, 1979, pp. R145-149.

7. Barenblatt, G.I., "The Mathematical Theory of Equilibrium Cracks in Brittle Fracture," in Advances in Applied Mechanics, Vol. VII, Academic Press, New York, 1962, pp. 59-129.

8. Dugdale, D.S., "Yielding of Steel Sheets Containing Slits," J. Mech. Phys. Solids, 1960, Vol. 8, pp. 100-104.

9. Rice, J.R., "Plastic Yielding at Crack Tip," Proceedings of the 1st Int'l Conf. on Fracture, Vol. I, Sendai, Japan, T. Yokobori et al. (Eds.), Japanese Soc. for Strength and Fracture of Materials, Tokyo, 1966, pp. 283-308.

10. Goodier, J.N. and Field, F.A., "Plastic Energy Dissipation in Crack Propagation," Fracture of Solids, D.C. Drucker and J.J. Gilman (Eds.), Wiley (Interscience), New York, 1963, pp. 103-118.

11. Donald, A.M. and Kramer, E.J., "The Entanglement Network and Craze Micromechanics in Glassy Polymers," J. Polymer Sci., Polymer Physics Edition, Vol. 20, 1982, pp. 1129-1141.

12. Wang, W.V., and Kramer, E.J., "A Distributed Dislocation Stress Analysis for Crazes and Plastic Zones at Crack Tips," J. Mat. Sci, Vol. 17, 1982, pp. 2013-2026.

13. Kramer, E.J. and Hart, E.W., "Theory of Slow, Steady State Crack Growth in Polymer Glasses," Polymer, Vol. 25, 1984, pp. 1667-1678.

8. FIGURE CAPTIONS

Figure 1. Problem definitions

Figure 2. The Barenblatt-Dugdale model.

Figure 3. p-v models used in the nonlinear craze and crack propagation studies in Sections 3 and 4. All models have the same γ .

Figure 4. Craze and crack propagation simulations for p-v model #6: Displacement profiles.

Figure 5. Craze and crack propagation simulations for p-v model #6: Stress distribution profiles.

Figure 6. The craze zone ω as a function of 'a' for various nonlinear p-v models (p-v models as indicated).

Figure 7. $\frac{\sigma_\infty}{p_m}$ as a function of c for various nonlinear p-v models (p-v models as indicated).

Figure 8. The rate of plastic work dissipation $\frac{\partial U_c}{\partial a}$ as a function of 'a' for various nonlinear p-v models (p-v models as indicated).

Figure 9. Craze growth initiating from a precut crack
(a) Initial precut crack, no far-field loading.
(b) Increasing far-field loading, no crack growth.
(c) Critical CTOD reached, crack growth imminent.

Figure 10. $\frac{\sigma_\infty}{p_m}$ as a function of c for a_o = 0.6, 0.9, 1.2, and 1.5 for the Barenblatt-Dugdale model 'D'.

Figure 11. $\frac{\sigma_\infty}{p_m}$ as a function of c for a_o = 0.3, 0.6, 0.9, 1.2, and 1.5 for p-v model #5.

Figure 12. $\frac{\sigma_\infty}{p_m}$ as a function of c for a_o = 0.3, 0.6, and 0.9 for p-v model #5 (enlargement of a part of Figure 11).

Figure 13. $\frac{\sigma_\infty}{p_m}$ as a function of c for a_o = 1.0, 1.2, 1.4, 1.6, and 1.8 for p-v model #6.

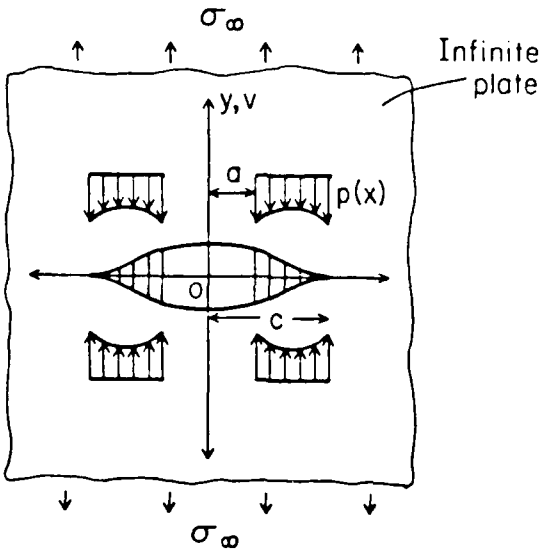

Figure 1. Problem definitions.

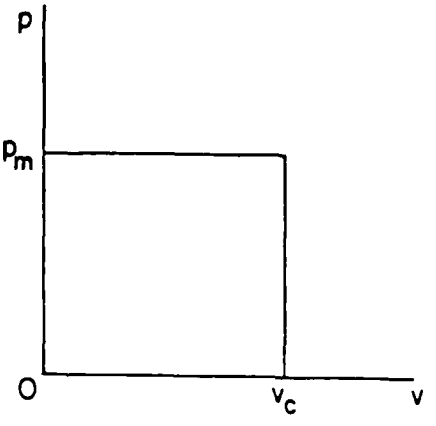

Figure 2. The Barenblatt-Dugdale model.

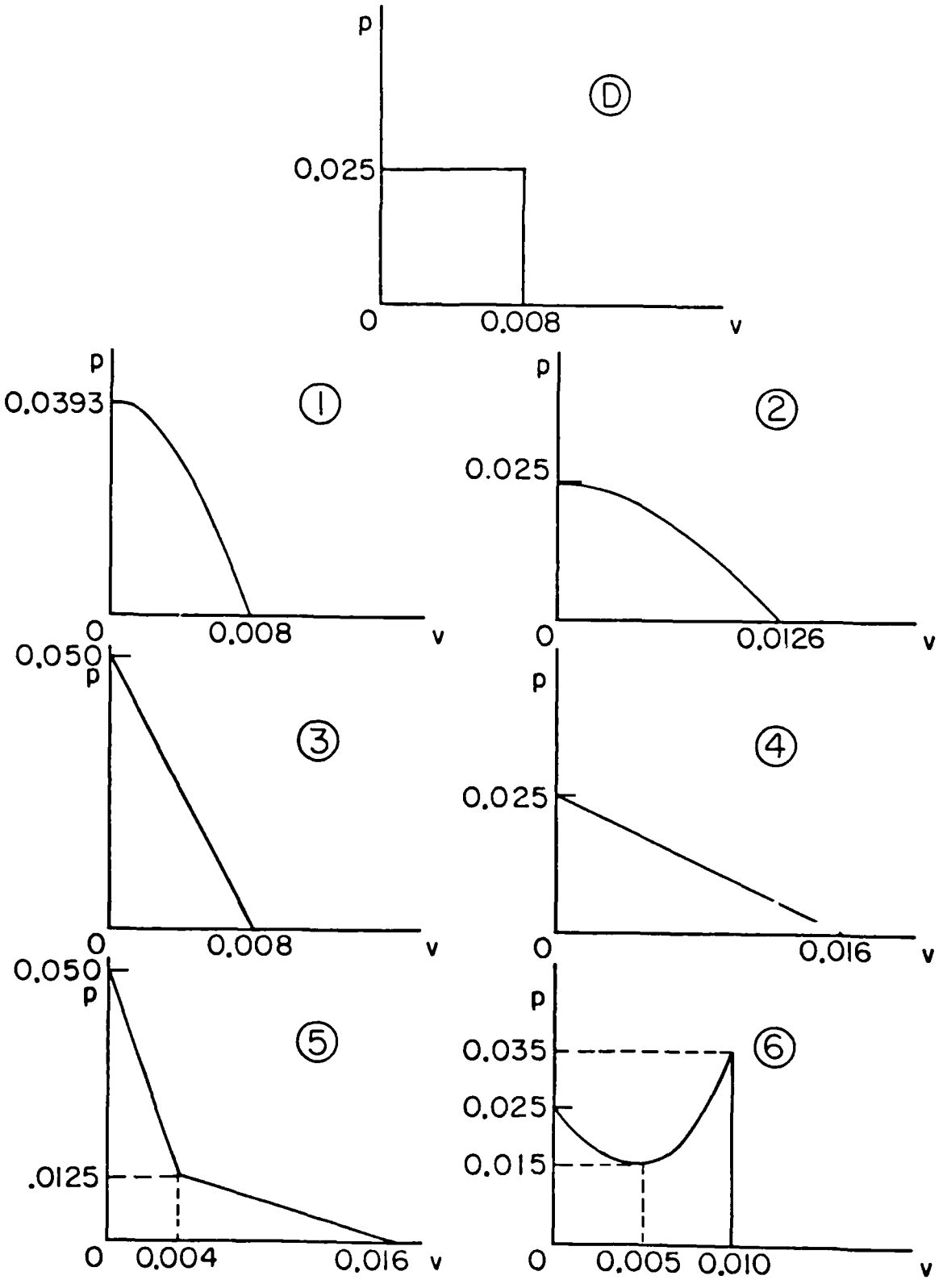

Figure 3. p-v models used in the nonlinear craze and crack propagation studies in Sections 3 and 4. All models have the same γ .

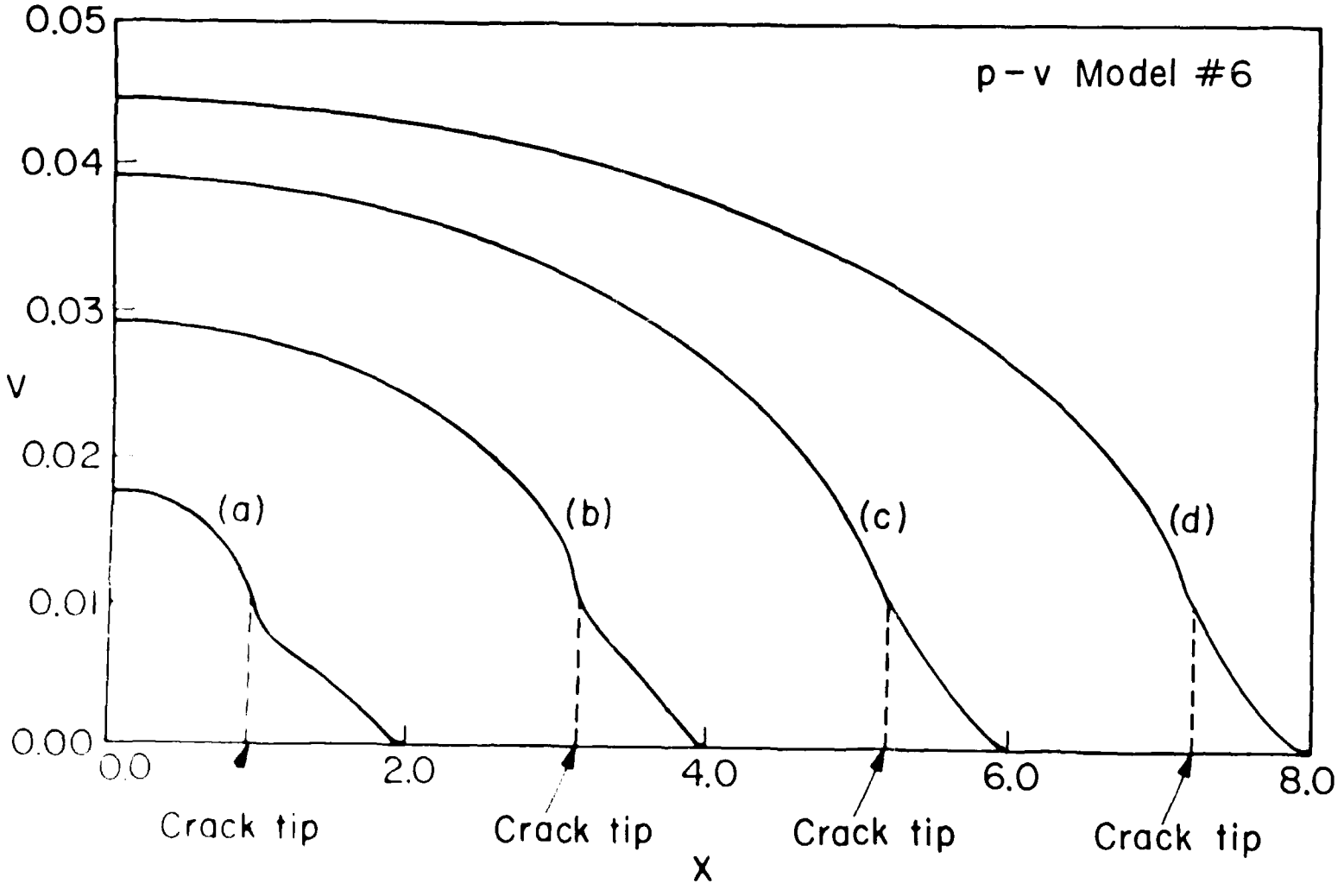

Craze and crack propagation simulations for p-v model #6: Displacement profiles

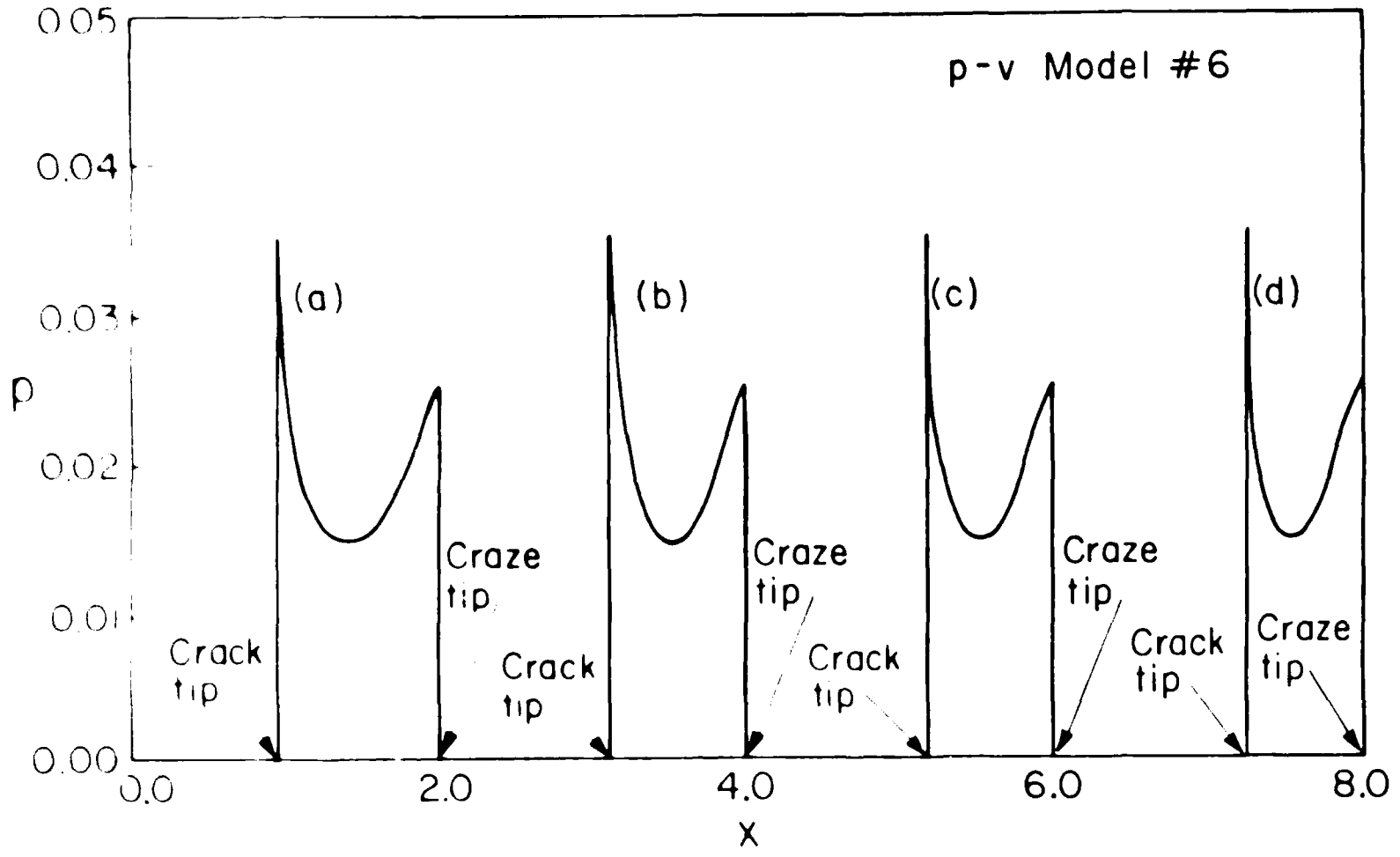

Craze and crack propagation simulations for p-v model #6 stress distribution profiles

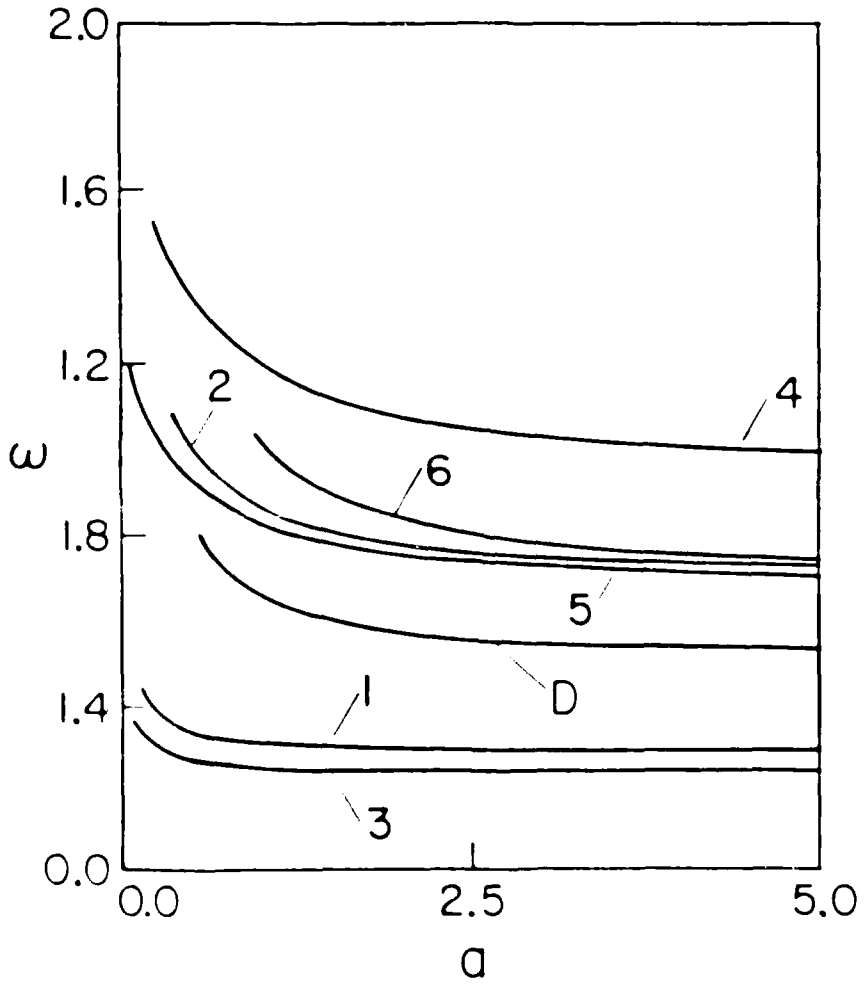

[illegible] The wave zone ω as a function of a for various nonlinear p-v models (p-v models as indicated)

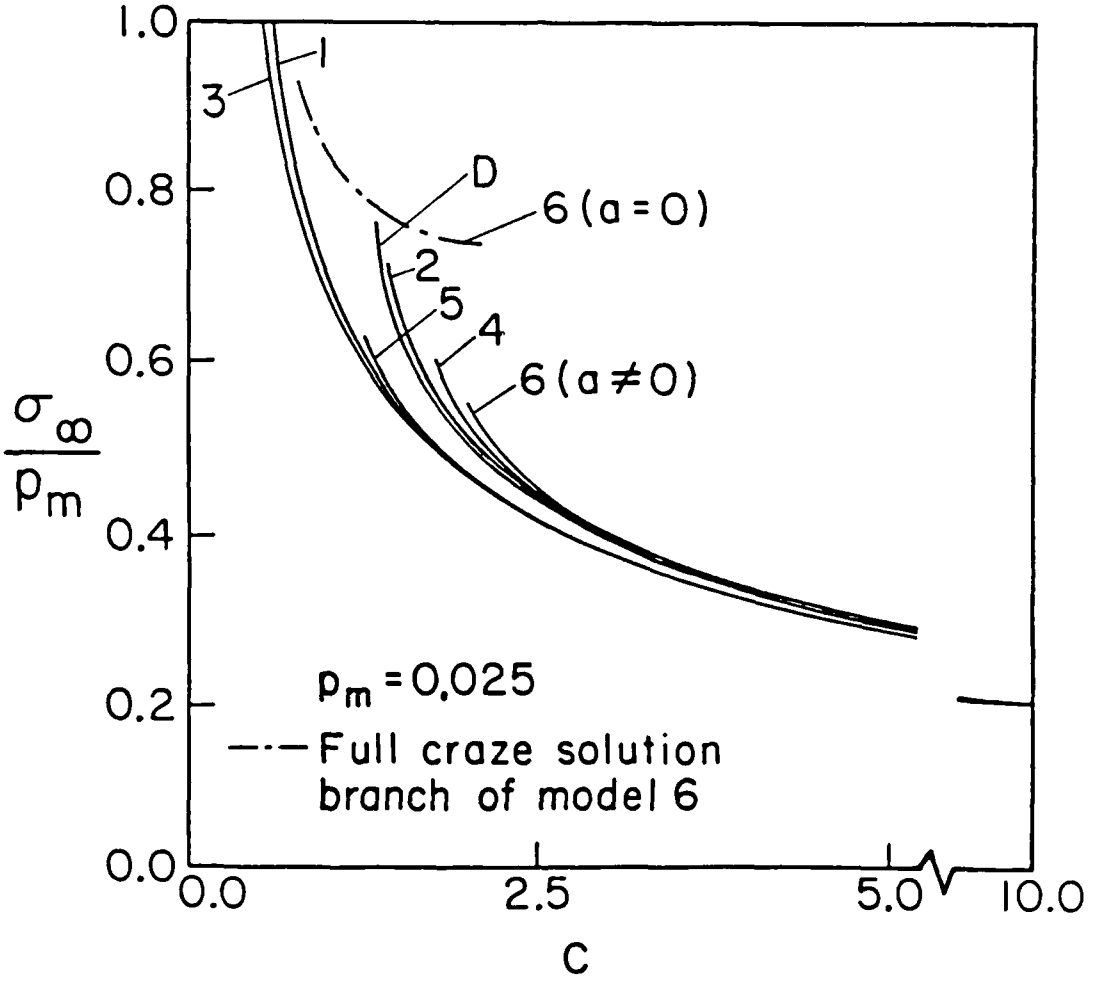

Figure 7. $\frac{\sigma_\infty}{p_m}$ as a function of c for various nonlinear p-v models (p-v models as indicated).

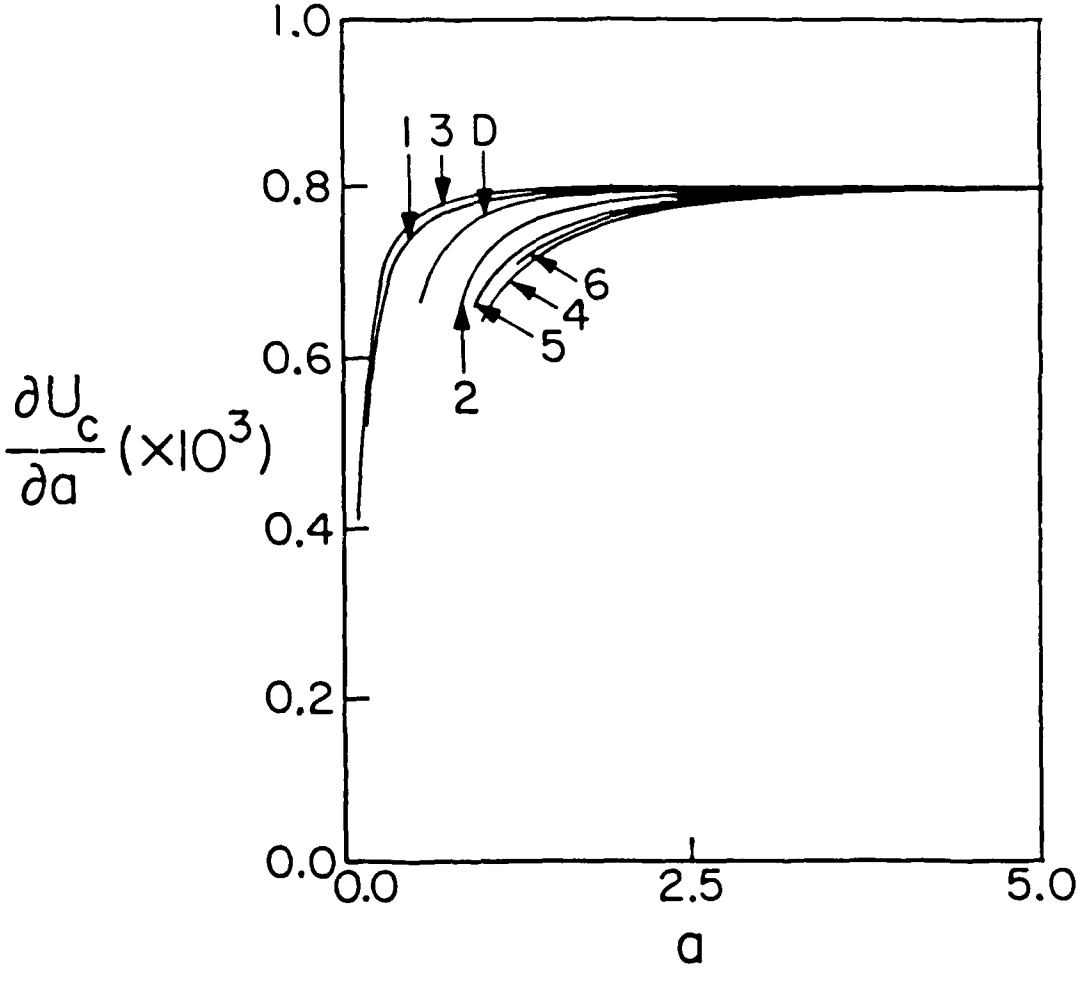

Figure 8. The rate of plastic work dissipation $\frac{\partial U_c}{\partial a}$ as a function of 'a' for various nonlinear p-v models (p-v models as indicated).

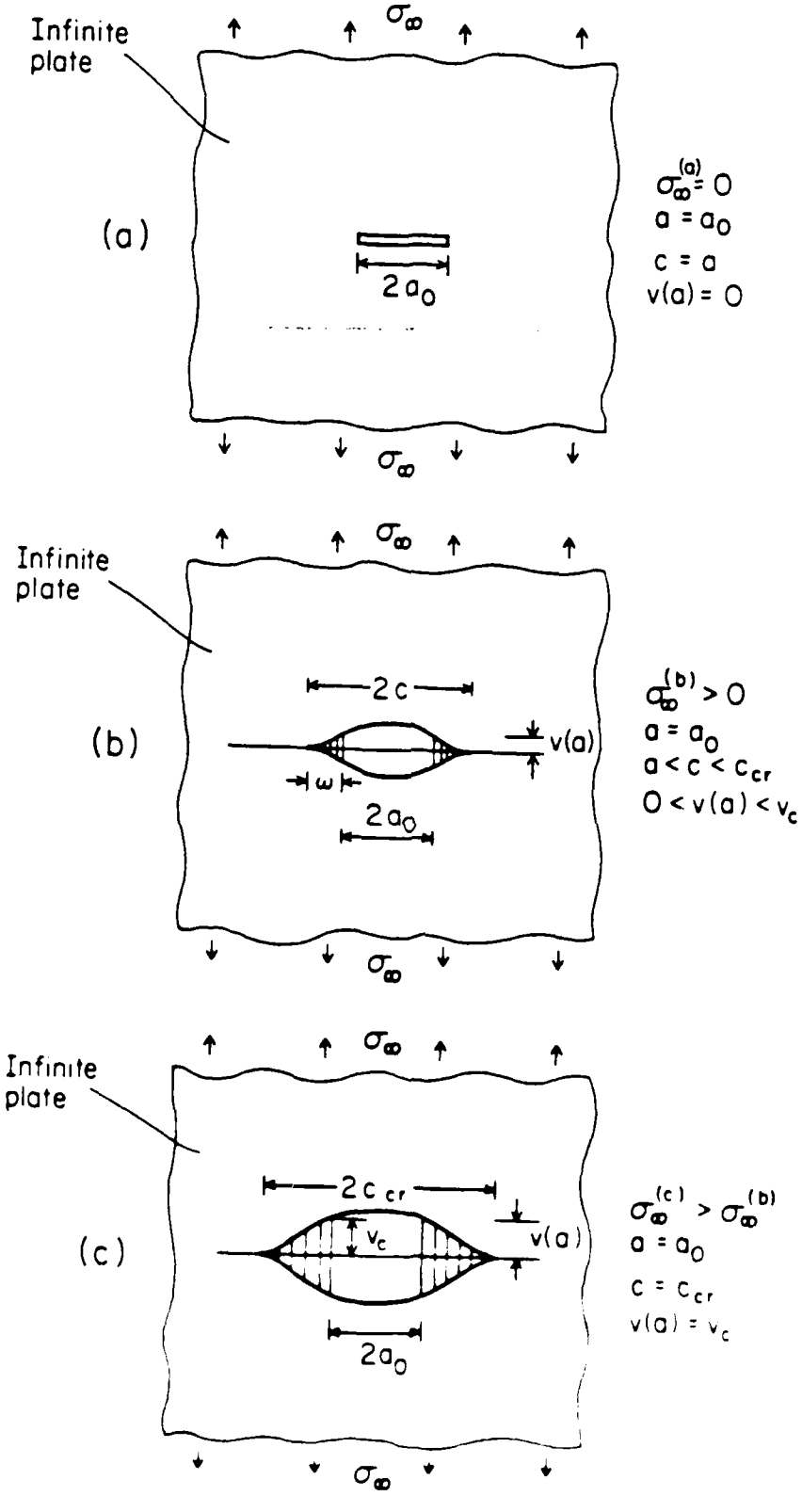

Figure 9 Craze growth initiating from a precut crack
(a) Initial precut crack, no far field loading
(b) Increasing far field loading, no crack growth
(c) Critical CTOD reached, crack growth imminent

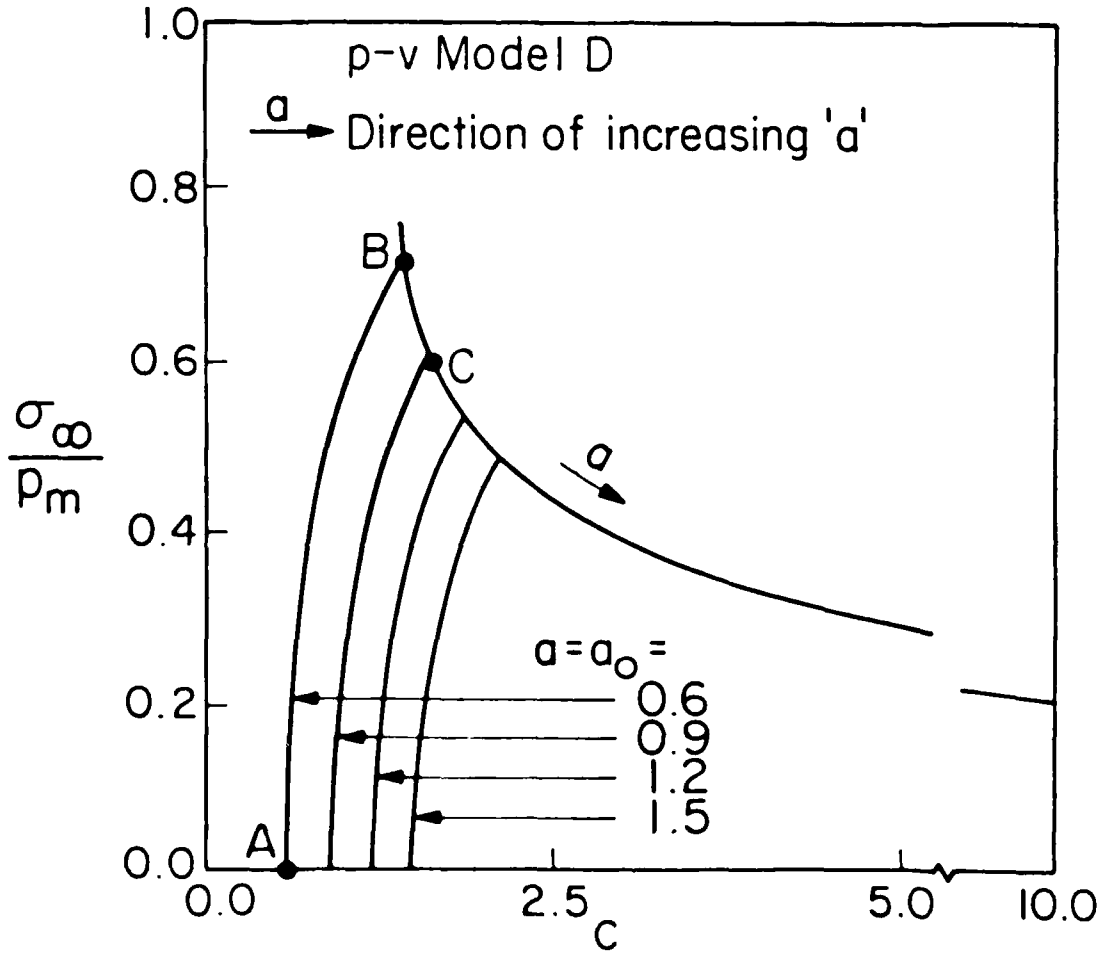

Figure 10 $\frac{\sigma_\infty}{p_m}$ as a function of c for a_o = 0.6, 0.9, 1.2 and 1.5 for the Barenblatt-Dugdale model D

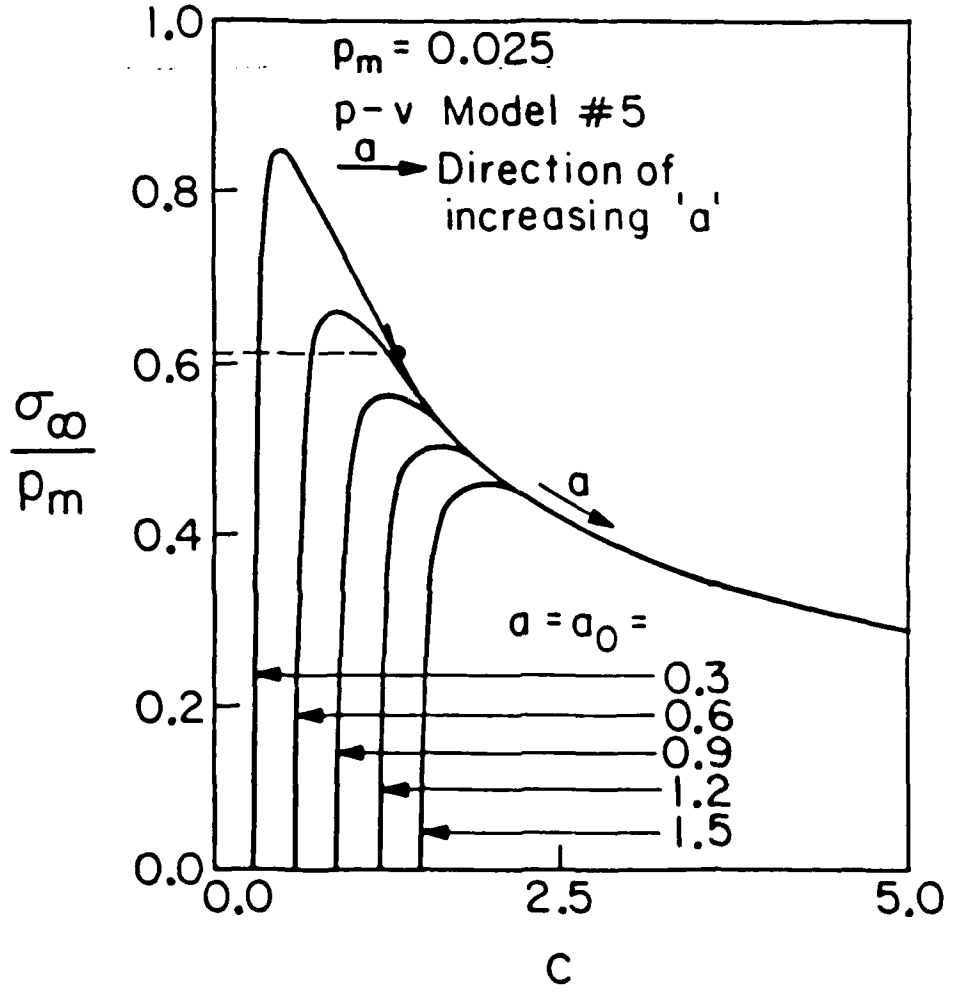

Figure 11. $\frac{\sigma_\infty}{p_m}$ as a function of c for a_0 = 0.3, 0.6, 0.9, 1.2, and 1.5 for p-v model #5

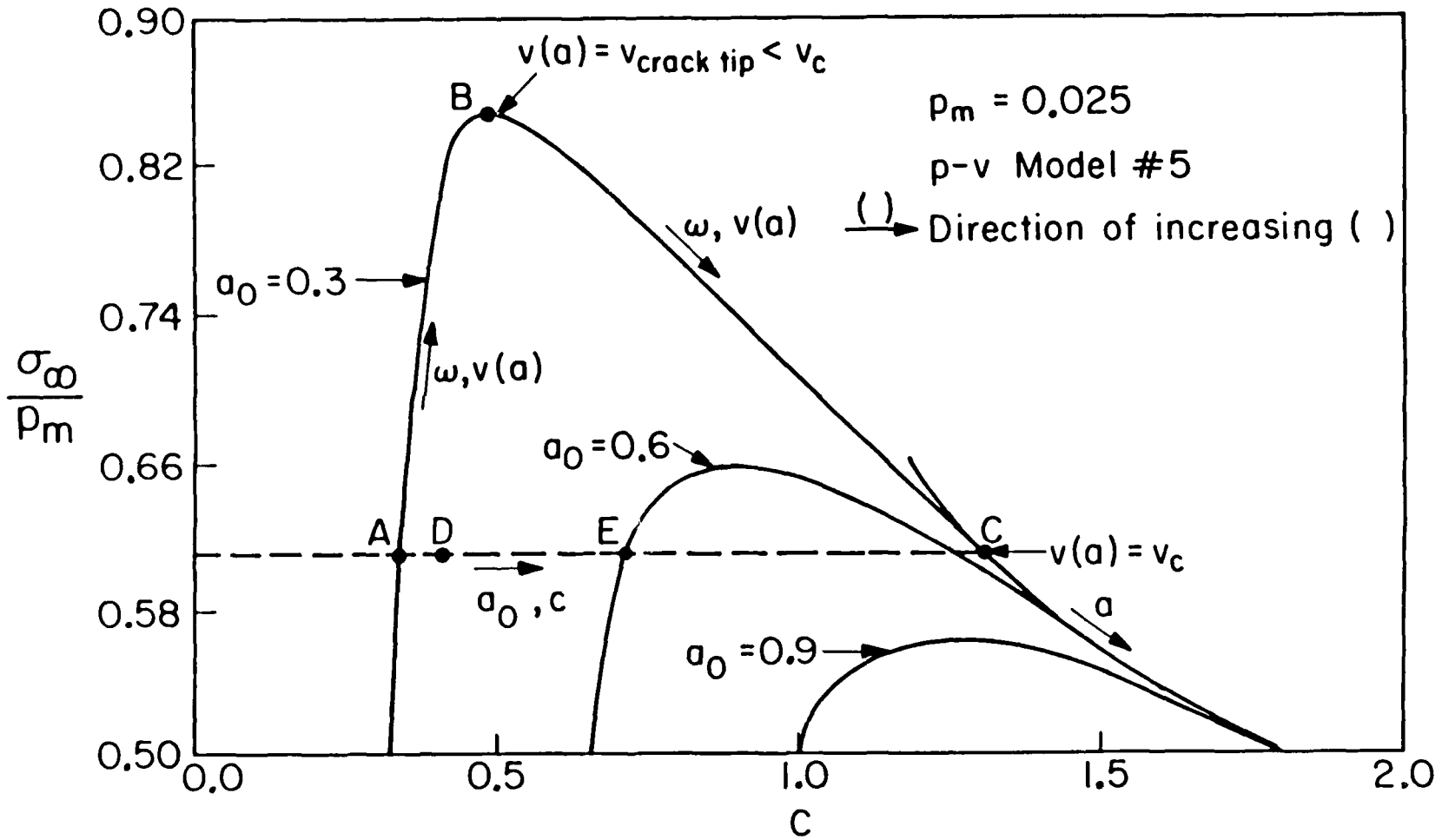

Figure 12. $\frac{\sigma_\infty}{p_m}$ as a function of c for a_o = 0.3, 0.6, and 0.9 for p-v model #5 (enlargement of a part of Figure 11).

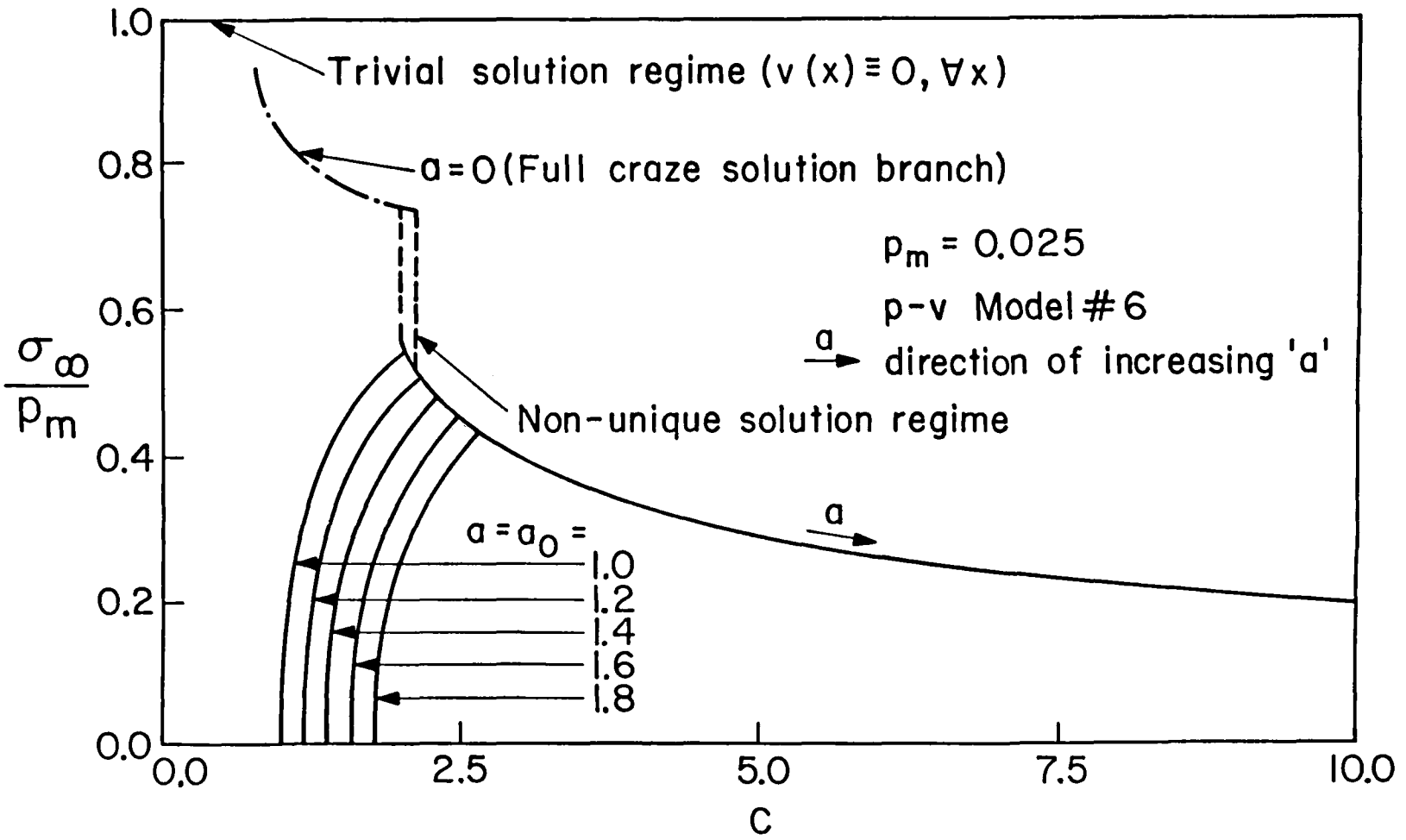

Figure 13. $\frac{\sigma_\infty}{p_m}$ as a function of c for a_o = 1.0, 1.2, 1.4, 1.6, and 1.8 for p-v model #6.

END

3-87

DTIC